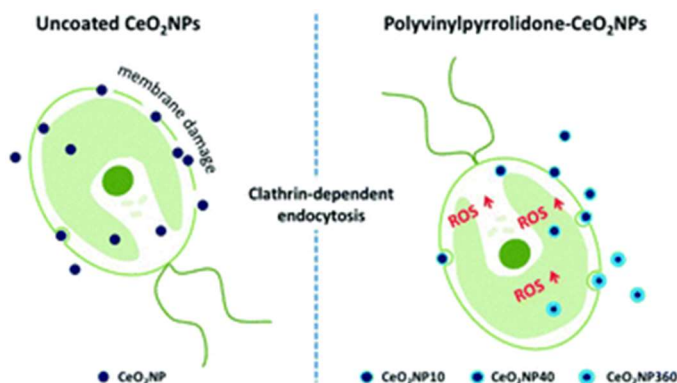


Internalization and toxicological mechanisms of uncoated and PVP-coated cerium oxide nanoparticles in the freshwater alga *Chlamydomonas reinhardtii*

This version is made available in accordance with publisher policies.

Please, cite as follows:

Gerardo Pulido-Reyes, Sophie Marie Briffa, Jara Hurtado-Gallego, Tetyana Yudina, Francisco Leganés, Victor Puentes, Eugenia Valsami-Jones, Roberto Rosal, Francisca Fernández-Piñas, Internalization and toxicological mechanisms of uncoated and PVP-coated cerium oxide nanoparticles in the freshwater alga *Chlamydomonas reinhardtii*, *Environmental Science: Nano*, 2019, <https://doi.org/10.1039/C9EN00363K>.



Internalization and toxicological mechanisms of uncoated and PVP-coated cerium oxide nanoparticles in the freshwater alga *Chlamydomonas reinhardtii*

Gerardo Pulido-Reyes^{1,*}, Sophie Marie Briffa², Jara Hurtado-Gallego¹, Tetyana Yudina³, Francisco Leganés¹, Victor Puentes³, Eugenia Valsami-Jones^b, Roberto Rosal^d, Francisca Fernández-Piñas¹

1 Departamento de Biología, Facultad de Ciencias, Universidad Autónoma de Madrid, Spain

2 School of Geography, Earth and Environmental Sciences, University of Birmingham, Birmingham, UK

3 Department Ciències Fisiològiques I, University of Barcelona, Barcelona, Spain

4 Departamento de Ingeniería Química, Universidad de Alcalá, Alcalá de Henares, Spain

* Corresponding author: gerardo.pulido@uam.es

Abstract

Due to the wide range of applications of cerium oxide nanoparticles (CeO₂NPs), a risk assessment of their biological effects using environmentally relevant species becomes highly important. There are contradictory reports on the effects of CeO₂NPs, which may be related to the use of different types of nanoparticles (NPs) and coatings. CeO₂NPs may act as an oxidant causing toxicity or as an antioxidant able to scavenge free radicals. As a consequence of such complexity, the toxicological behaviour of these NPs is still poorly understood. Moreover, little is known about the internalization process of CeO₂NPs in algae. There is evidence of CeO₂NPs-internalization by the green alga *Chlamydomonas reinhardtii*, but the mechanism and route of uptake are still unknown. In this study, we used an uncoated and different polyvinylpyrrolidone (PVP)-coated CeO₂NPs with the aim of identifying their toxicological mechanisms to *C. reinhardtii* and exploring their possible internalization. Our results showed that PVP coated-CeO₂NPs significantly increased the formation of reactive oxygen species in exposed cells, indicating that oxidative stress is an important toxicity mechanism for these particles. Direct contact and damage of the cellular membrane was identified as the mechanism causing the toxicity of uncoated NPs. From experiments with endocytosis inhibitors, clathrin-dependent endocytosis was revealed as the main internalization route for all NPs. However, as uncoated CeO₂NPs led to severe cellular membrane damage, direct passage of NPs through membrane holes could not be discarded. To our knowledge, this is the first report with evidences of direct linking between NP internalization and a specific endocytic pathway. The results presented here will help to unravel the toxicological mechanism and behaviour of CeO₂NPs and provide input information for the Environmental Health and Safety assessment of CeO₂NPs.

Introduction

Surface coatings of NPs are applied to selectively change or influence several particle properties¹. The surface of a particle can be covered with a wide variety of elements such as dendrimers², polymers³, metal⁴, metalloid⁵, peptides⁶ or polysaccharides⁷. The increase of particle stability⁸, the prevention of particle core dissolution⁸, the protection of particle functionality or the enhancement of biocompatibility⁹ are some different purposes to use these coatings. However, since coatings change the surface and physicochemical properties of NPs in comparison with bare NPs, it is essential to completely study the implications of their use, giving that they may have an important role on how coated NPs interact with biological systems and, therefore, on their (eco)toxicological effects.

Cerium oxide nanoparticles (CeO₂NPs) have become an exceptionally versatile material due to their high surface area and redox activity^{10, 11}. A diversity of applications has emerged due to their singular surface

chemistry. Applications include electrochemical biosensors¹², radiation protector¹³, corrosion-resistant coatings¹⁴ and antioxidant agents in the biomedical field¹⁵⁻¹⁷, among others¹¹. Controlling the surface properties of CeO₂NPs is essential for them to behave as designed. The reactivity of CeO₂NPs strongly depends on NP size. However, it has also been shown that surface coatings play a significant role¹⁸. In recent years, CeO₂NPs have been synthesized and functionalized with a variety of molecules such as small ligands¹⁹, polymers²⁰⁻²², surfactants²³ and other organic molecules²⁴ using different strategies²⁵.

Due to their variety of applications and extensive use, CeO₂NPs may be released to the aquatic environment, where the interaction with aquatic organisms is unavoidable. Until now, several authors showed that CeO₂NPs may cause some harmful effects in different environmentally relevant microorganisms²⁶⁻²⁹. Considerable efforts have been undertaken in order to understand the toxicological mechanisms of

CeO₂NPs^{28,30}, which is a difficult task due to the existence of contradictory results^{29,31-32}. It has been found that CeO₂NPs displays enzyme-mimicking activities^{15, 34, 35}, protecting against oxidative stress-induced cellular damages, but also they have showed toxic effects to different organisms and cell lines³⁶⁻³⁸. Moreover, although some authors have shown their skepticism about particle internalization in algal cells³⁹, it has been recently revealed that internalization processes might be involved in the effects of CeO₂NPs in the model aquatic algae *Chlamydomonas reinhardtii* (*C. reinhardtii*)⁴⁰. However, it is unclear how CeO₂NPs can pass through cell envelopes. Overall, whether CeO₂NPs are internalized in green algae by using some endocytic routes or by using other mechanisms is not fully understood. Further research is also needed on the effect of coatings on toxicity and NP uptake. In this regard, some results point towards an enhanced internalization of nanomaterials with organic coatings⁴⁰⁻⁴².

Furthermore, the biological effect of coatings on the toxicity of CeO₂NPs to environmentally relevant microorganisms has not been completely assessed. On the one hand, several authors have found that uncoated CeO₂NPs are more toxic than citrate-coated NPs towards a snail⁴³ and amphibian larvae⁴⁴. On the other hand, it has been shown that poly(acrylic acid)-stabilised CeO₂NPs were more toxic than pristine forms to model alga *Pseudokirchneriella subcapitata*⁴⁵. Either way, whether CeO₂NPs are being synthesized with coatings to enhance their colloidal stability or to develop new functionalities, they thus should be evaluated with those coatings as they will be possibly found in the environment in that form. In this study, we used bare and PVP-coated CeO₂NPs with the aim of identifying the mechanism by which they affect the green algae *C. reinhardtii*. Attention was also centered on the impact of different coatings and on the potential routes of uptake and internalization.

Materials and methods

Synthesis of CeO₂NPs

Three PVP capped CeO₂NPs were synthesized using the method described by Briffa et al²². Briefly, 130 mg of Ce(NO₃)₃ were dissolved in a 5 mM solution of PVP, with different molecular weights (10, 40 and 360 kDa). The mixture was heated for 3 h at 105 °C, after which the reaction was quenched and excess PVP was removed using acetone. Centrifuging at 4000 rpm at room temperature for 10 minutes resulted in a yellow pellet that was retained and resuspended in ultra-high purity water. CeO₂NPs without coating were also prepared as follows. 4 nm CeO₂NPs were synthesized by the chemical precipitation of Ce(NO₃)₃ · 6H₂O (Sigma-Aldrich, St. Louis, MO, USA) in a basic

aqueous solution⁴⁶. In this method, 10 mM of Ce(NO₃)₃ · 6H₂O is dissolved in 100 mL of MilliQ H₂O at room temperature. Next, 1 mL of tetramethylammonium hydroxide (TMAOH, 1.0 ± 0.02 M in H₂O) is added, and the mixture is left under stirring for 24 hours. Afterwards, purification of NPs is carried out by centrifugation and resuspension in a solution of 1 mM TMAOH, which act as a stabilizer. CeO₂NPs were kept at 4 °C until administration.

Characterization of CeO₂NPs suspension

Transmission Microscopy (TEM) was used to analyse size and morphology of the particles. X-ray diffraction of nanoparticles were analysed to determine their crystallinity; surface chemistry (Ce³⁺/Ce⁴⁺) ratios on the surface of CeO₂NPs was analysed using X-Ray photoelectron spectroscopy as previously described by Deshpande et al⁴⁷. The amount of the PVP on the coated CeO₂NPs was quantified by thermogravimetric analysis (TGA), using a PerkinElmer TGA 8000TM Thermogravimetric analyser, performed under nitrogen flow (60 mL/min) from 40 to 1146 °C, with a 5 °C/min heating rate. Moreover, the optical properties were analysed using Ultraviolet–Visible Spectrophotometer (PerkinElmer, Lambda 750 S, 60 mm Int. Sphere). The same instrument was used for analysing the optical properties of CeO₂NPs in the biological media. Hydrodynamic diameter and ζ-potential of the CeO₂NPs suspensions in the different assay conditions were measured by Dynamic light scattering (DLS) and electrophoretic light scattering, respectively, using a Zetasizer Nano ZS particle size analyser from Malvern Instruments Ltd. (Malvern, United Kingdom) essentially as described elsewhere⁴⁸. Colloidal stability was measured both in distilled water and algal culture medium (six times diluted Tris-Acetate-Phosphate, TAP/6⁴⁹).

Biological end-points

The unicellular green alga *C. reinhardtii* Dangeard (strain CCAP 11/32A mt +) was obtained from the Culture Collection of Algae and Protozoa of Dunstaffnage Marine Laboratory (Scotland, UK). Growth inhibition experiments using *C. reinhardtii* were performed in TAP/6 medium as described in the standard OECD TG 201⁵⁰. Exposure experiments to CeO₂NPs suspensions were carried out in 12 mL of TAP/6 culture medium in 25 mL flasks. Growth inhibition experiments were performed for 72 h under the same experimental conditions using a set of serial dilutions at least in triplicate. The effect of CeO₂NPs on the growth of microalgae was assessed by measuring the optical density at 750 nm after 72 h of exposure. *In vivo* fluorescence of chlorophyll *a* (Ch *a*) was also measured as a key parameter of photosynthesis status after 24 h of exposure. 100 µL of each sample was

transferred to an opaque black 96-well microtiter plate and fluorescence of chlorophyll *a* was recorded with 485/645 excitation/emission wavelengths on a Synergy HT multimode microplate reader (BioTek, Seattle, WA).

Flow cytometric (FCM) analyses

FCM analyses of *C. reinhardtii* cells were performed on a Cytomix FL500 MPL flow cytometer equipped with an argon-ion excitation wavelength (488 nm), detector of forward (FS) and side (SS) light scatter and four fluorescence detectors (Beckman Coulter Inc., Fullerton, CA, USA), as described previously²⁸. The intracellular reactive oxygen species (ROS), superoxide anion and hydrogen peroxide produced by *C. reinhardtii* were measured by means of the cell permeable fluorescent dye dihydrorhodamine 123 (DHR 123) and hydroethidine (HE), respectively. MitoTracker Orange CM-H₂TMRos (Invitrogen Molecular Probes) was used to target mitochondria and evaluate possible alterations of mitochondrial ROS homeostasis. The level of cellular lipid peroxidation was evaluated with C₄,C₉-BODIPY[®]. Changes in cytoplasmic membrane potential were evaluated with the probe DiBAC₄(3). FCM was also used to detect cells with cell membrane damage by using the fluorescent probe Propidium Iodide (PI) and cells with altered metabolic activity by using Fluorescein Diacetate (FDA). FDA is a non-polar, hydrophobic, non-fluorescent esterified compound which readily permeates the cell membrane and is hydrolysed by non-specific esterases, leaving the fluorescent by-product fluorescein. Therefore, fluorescein is accumulated by active cells and it has been previously shown as a rapid and effective technique to assess microalgae metabolic activity^{51, 52}. Data acquisition was performed using MXP-2.2 software, and the analyses were performed using the Flowing 2.5.1 software. Fluorescence was analysed in Log mode. Cells were incubated with the appropriate fluorochrome for each parameter at room temperature and in the dark, after 24 h of CeO₂NPs exposure, prior to FCM analyses. All fluorochrome stock solutions were prepared in dimethyl sulfoxide (DMSO) and stored at -20 °C, except for the solution of propidium iodide (PI), which was made in ddH₂O and stored at 4 °C. The fluorochrome concentrations and incubation times were as reported elsewhere⁵³ and can be found in the Electronic Supplementary Information (ESI) Table S1. Three independent experiments with triplicate samples were carried out for each parameter.

Internalization studies

To determine the amount of CeO₂NPs inside cells, the algal cells were incubated with 10 mg/L CeO₂NPs for 12 h and 48 h. Then, they were collected by centrifugation (4000 rpm) and the supernatant was

recovered to determine the amount of free suspended CeO₂NPs. 20 mM EDTA was used to remove the CeO₂NPs bound onto the cell wall⁵⁴ and the samples were again centrifuged. This process was repeated three times and the supernatant was used to calculate the content of CeO₂NPs measured as Ce bound to the algal cells (this method was certainly effective as no nanoparticles attached to the cell envelopes were observed nor detected by Transmission Electron Microscopy coupled with X-Ray Energy Dispersive Spectroscopy (TEM-XEDS) after the washing steps, see ESI Figure S1; however, it is worth noting that the presence of Ce at very low concentrations cannot be discarded as there might be still some Ce that could not be detected by this technique due to its detection limit⁵⁵). The remaining algal pellet was acid-digested for 12 h to calculate the intracellular Ce. The Ce content in all samples was measured by Inductively Coupled Plasma Mass Spectrometry (ICP-MS) on an ICP-MS NexION 300XX from Perkin-Elmer. Moreover, in other set of experiments, algal cells were incubated 30 min with sodium azide (NaN₃; 0.25 mM), monodansylcadaverine (MDC; 0.2 mM), 5-(N-ethyl-N-isopropyl)-amiloride (EIPA; 10 μM) and filipin complex^{56, 57} during 30 min before NP exposure in order to block the different endocytic routes and evaluate the impact of endocytosis on CeO₂NPs internalization and toxic effects through the photosynthetic parameter of Ch *a* fluorescence. A time period of 12 h was chosen to assess the endocytosis of algae under a healthy condition as described by Wang et al⁵⁸. ICP-MS was also used for the intracellular determination of CeO₂NPs after the treatment with MDC. For TEM analysis, algal cell suspensions exposed to CeO₂NPs before and after EDTA treatment were collected by centrifugation (4000 rpm during 4 min) and prepared as described elsewhere⁴⁸. Briefly, cells were fixed with glutaraldehyde (3.1%; phosphate buffer, pH 7.2) in agar blocks for 3 h at 4 °C. Post-fixation was performed with osmium tetroxide in phosphate buffer for 2 h at 4 °C. Samples were dehydrated in ethanol and embedded in Durcupan resin and, then, sectioned in a Leica Reichert Ultracut S ultramicrotome, stained with uranyl acetate 2%. Ultrathin sections were visualized on a JEOL (JEM 1010) electron microscope (100 kV) or on a JEOL JEM 2100 (200 kV) coupled with XEDS. All reagents used for TEM preparations were Electron Microscopy grade.

Gene expression

Gene expression studies were carried out by the Genomics Unit of the Madrid Science Park (Madrid, Spain). Briefly, total RNA from control and CeO₂NPs samples were extracted from frozen cell pellets using RNeasy Mini kit (Qiagen). Remaining genomic DNA was removed using RQ1

RNase-Free DNase (Promega) for 30 min at 37 °C. The concentration of RNA was spectrophotometrically determined in a Nanodrop (Thermo Scientific). First-strand cDNA was synthesized from 250 ng of total RNA using the High Capacity cDNA Archive Kit (Applied Biosystems, Thermo Fisher). Real-time PCR of selected genes was performed using SYBR Green[®] in an AB fast-7900HT System (Applied Biosystems, Thermo Fisher) under standard running conditions. The selected genes were *16S*, a constitutively expressed control gene, and *CHC1*, a gene in *C. reinhardtii* thought to be involved in clathrin-mediated endocytosis⁵⁹. RT-qPCR primer used in this study were 18Sf (GCCTAGTAAGCGCGAGTCAT), 18Sr (AGCCAAGCTCAATCCGAACA), CHC1f (CAGCGCGGACAGTGCCCTCAT) and CHC1r (TGCCTTCAGCTTCGTTTTGGTGTC), which were designed using the DNASTAR's Lasergene software. The 2^{-ΔΔC} scheme was used to normalize and calibrate transcript values relative to the 18S gene using RQ Manager Software (Applied Biosystems)⁶⁰.

Table 1. Physicochemical properties of the tested CeO₂NPs in algal culture medium.

Sample Name	PVP chain length	ζ -Pot (mV)	DLS Diameter (nm)	PDI*
CeO ₂ NP	-	-13.0 ± 1.1	10.2 ± 0.5	0.38
CeO ₂ NP10	10 kDa	-8.1 ± 0.8	6.0 ± 0.1	0.18
CeO ₂ NP40	40 kDa	-7.3 ± 0.4	8.2 ± 0.6	0.15
CeO ₂ NP360	360 kDa	-9.2 ± 0.3	12.5 ± 0.1	0.28

* Polydispersity Index

Statistical Analysis

Means and standard deviation values were calculated for each treatment from three independent replicate experiments. Statistical analyses were performed by using R software 3.0.2 (The R Foundation for Statistical Computing[®]) and Rcmdr 2.0–4 package. A one-way ANOVA coupled with Tukey's HSD (honestly significant difference) post-hoc test was performed for comparison of means. Statistically significant differences were considered to exist when $p < 0.05$.

Results

Physicochemical characterization of CeO₂NP

Three CeO₂NPs were synthesized with three different PVP molecular weight coatings (10 kDa, 40 kDa and 360 kDa). Accordingly, the CeO₂NPs were named CeO₂NP10, CeO₂NP40 or CeO₂NP360, depending on the PVP chain length. CeO₂NPs without coating were

referred to as CeO₂NP. A complete characterization of all CeO₂NPs used regarding size, morphology, crystallinity, optical properties, coating measurements and surface chemistry can be found in ESI Figure S2. CeO₂NP, CeO₂NP10, CeO₂NP40 and CeO₂NP360 had spherical shape with diameters approximately of 5, 5, 7 and 12 nm, respectively. Regarding crystallinity, it was not possible to add this information for capped CeO₂NP as the PVP capping agent interfered with the XRD measurements. However, it has been previously shown that CeO₂ nanorods and nanocubes have particular structure with {100}c and {110} + {100} facets, respectively⁶¹⁻⁶³, while spheres of CeO₂NPs show similar crystallinity properties, exposing the characteristic diffraction peak at $2\theta = 28.51^\circ$ which correlate to {111} crystal plane⁶⁴. ESI Figure S2 also illustrates UV-visible absorbance spectra of all CeO₂NPs. NP surface chemistry (Ce³⁺/Ce⁴⁺ ratio) has been also included, since this property, among other important nanoparticle characteristics, has been recently revealed as a key factor of uncoated CeO₂NPs toxicity²⁸. CeO₂NP40 had the highest % surface Ce³⁺ (100 %) followed by CeO₂NP360 (81.3 %), while CeO₂NP and coated CeO₂NP10 showed similar % surface Ce³⁺ with 32 and 39 %, respectively. Table 1 shows the physicochemical characteristics of the four CeO₂NPs at 10 mg/L suspended in the algal culture medium (pH 7). The particles had a negative surface charge (ζ-potential) in TAP/6 with similar values from -7 to -13 mV. There was a slight increase in the effective diameter based on the PVP-chain length: 6.0 nm, 8.2 nm and 12.5 nm for CeO₂NP with 10 kDa-PVP, 40 kDa-PVP and 360 kDa-PVP, respectively; whereas the uncoated CeO₂NPs had a diameter size of 10.2 nm.

Toxicity of the CeO₂NPs towards *C. reinhardtii*: effect on growth and photosynthesis

The effect of the coated and uncoated CeO₂NPs towards *C. reinhardtii* is shown in Figure 1. Figure 1A shows the biological effect of 72 h exposure to CeO₂NPs on the growth of *C. reinhardtii* in the 0.1-50 mg/L range. CeO₂NP was more toxic at low concentrations (Minimum Inhibitory Concentration (MIC): 5 mg/L) than PVP-coated CeO₂NPs, irrespective of PVP molecular weight. However, CeO₂NP10 and CeO₂NP40 resulted in higher growth inhibition at 50 mg/L. As photosynthesis is a key process in this organism, we checked whether the photosynthetic machinery of *C. reinhardtii* was affected by CeO₂NPs by measuring the *in vivo* chlorophyll *a* (Ch *a*) fluorescence emission. There was a statistically significant increase in the Ch *a* fluorescence of all samples with respect to control levels clearly dependent on NP concentration. In this regard, the increase observed by all CeO₂NPs has been related with an interruption of the electron transport at the acceptor side

of the Photosystem II^{65, 66}. Interestingly, while PVP-CeO₂NPs induced photosynthetic alterations at concentrations as low as 1 mg/L, CeO₂NP did not cause any statistically significant effect until 10 mg/L. The toxicity of PVP without NPs and TMAOH (the agent used for the stabilization of uncoated NPs) was also investigated to account for any toxic effect. Concentrations higher than 100 mg/L and 2.5 mM,

respectively, were needed to induce a noticeable growth inhibition effect, supporting the previous results regarding the low toxic profile of these compounds^{67, 68} (ESI Figure S3 and S4). The results of growth inhibition together with the changes induced in the photosynthetic system suggested that coated and uncoated CeO₂NPs may display different biological toxic mechanisms to *C. reinhardtii*.

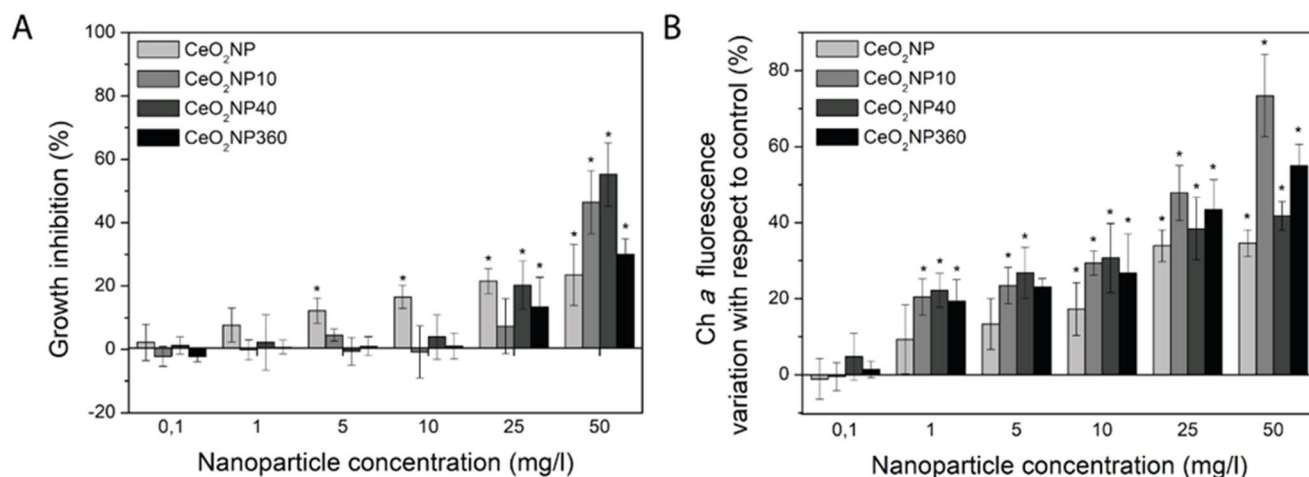


Figure 1. Effect of 72 h exposure to the four CeO₂NPs on the growth (A) and in vivo Ch a fluorescence of *C. reinhardtii*. Statistically significant differences ($p < 0.05$) are marked by asterisks. Ch a: chlorophyll a. Control values of Ch a fluorescence were in the range of 944.6 to 1094.1 arbitrary units (a. u.).

The effects of CeO₂NPs on relevant cellular biomarkers

Therefore, in order to clarify the mechanisms underlying the observed toxicity, several cytotoxicity biomarkers (cell membrane integrity, oxidative stress, metabolic activity and cytoplasmic membrane potential) were analysed by FCM after 24 h of exposure. Two different concentrations of CeO₂NPs were chosen: the highest predicted environmental concentration (as calculated by O'Brien et al (2011), 0.1 mg/L;⁶⁹) and also an effective NP concentration (10 mg/L), i.e. the concentration at which all CeO₂NPs significantly increased Ch a fluorescence.

The highest predicted environmental concentration of 0.1 mg/L did not produce any alteration in the analysed physiological parameters (see ESI Figure S5 and Figure S6). However, several alterations were observed with a concentration of 10 mg/L. To check whether the cytoplasmic membrane was damaged by CeO₂NPs, the fluorescent dye PI was used. The flow cytograms showed the presence of two distinct cell subpopulations, R1 and R2, in control cultures (Figure 2A). R1 comprised around 89 % of total cells and corresponded to intact cells (intact membranes). R2 subpopulation comprised cells with a basal level of damaged membranes (around 11 % of total cells). FCM results showed that only CeO₂NP significantly ($p <$

0.05) affected membrane integrity by increasing the R2 subpopulation to 21 %, indicating a clear damage to the cytoplasmic membrane. As uncoated CeO₂NPs were suspended in TMAOH, the effect of TMAOH on cytoplasmic membrane was also tested (ESI Figure S7). Neither TMAOH nor coated-CeO₂NPs displayed alterations in cytoplasmic membrane integrity.

The effect of CeO₂NPs on cytoplasmic membrane potential of *C. reinhardtii* was also studied by FCM using the fluorescent dye DIBAC₄(3) (Figure 2B). Flow cytograms of control cells showed two clear subpopulations (R1 and R2). R1 was the largest one comprising around 96 % of total cells while the R2 subpopulation (showing a slight membrane depolarization) accounted for 4.2 % of total control cells. CeO₂NP, CeO₂NPs10 and CeO₂NPs40 considerably increased membrane depolarization by 13.1 %, 27.4 % and 36.9 % of total cells (R2 subpopulation; Figure 2B), respectively. CeO₂NPs360 did not have any significant effect on this parameter. Furthermore, as shown in Figure 2C, the percentage of metabolically non-active cells (R2), determined by flow cytometry using FDA, increased significantly ($p < 0.05$) in cultures exposed to all treatments, in comparison with control levels. However, CeO₂NPs10 and CeO₂NPs40 had the highest percentages with 34 % and 35 % of total cells with a lower metabolic activity.

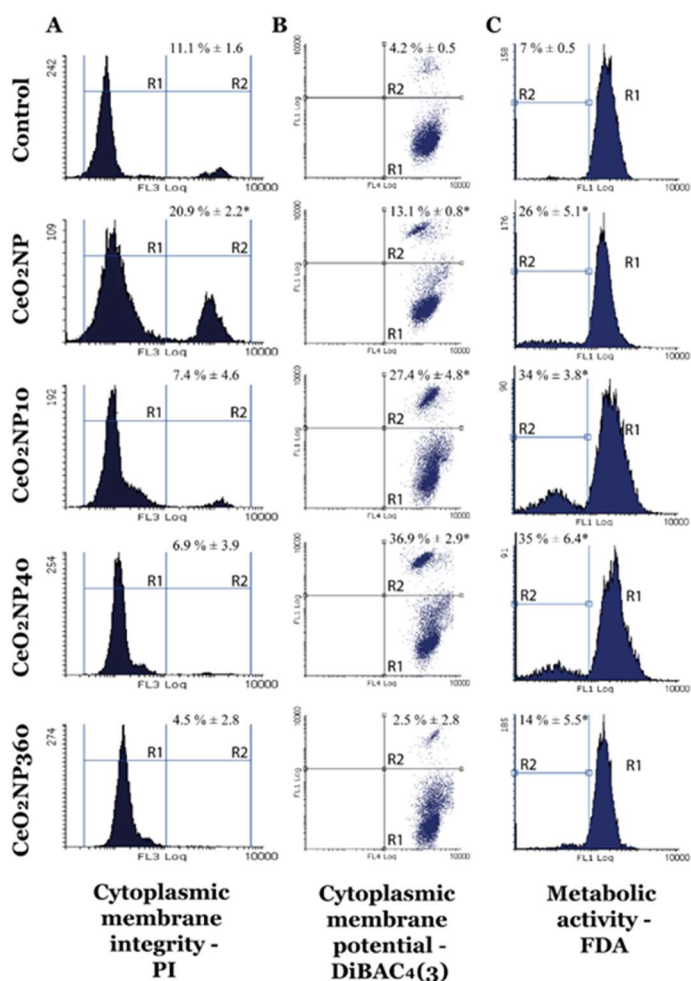


Figure 2. Effect of CeO₂NPs on cytoplasmic membrane integrity (A), cytoplasmic membrane potential (B) and metabolic activity (C) of *C. reinhardtii* by FCM, using the fluorochromes PI, DiBAC4(3) and FDA, respectively. Statistically significant differences ($p < 0.05$) are marked by asterisks.

The production of intracellular ROS in exposed cells has been identified as an important toxicity mechanism for CeO₂NPs^{28, 70}. The fluorescent indicators HE and DHR123 were used to determine intracellular superoxide anion (O₂^{•-}) and H₂O₂, respectively (Figure 3A and 3B). The CeO₂NPs coated with PVP (CeO₂NPs10, CeO₂NPs40 and CeO₂NPs360) caused a significant increase in the intracellular level of both oxidant species, while CeO₂NP did not produce any alteration. CeO₂NPs40 led to the highest level of intracellular hydrogen peroxide formation (Figure 3B). The alterations of mitochondrial ROS homeostasis and cellular lipid peroxidation were revealed by MitoTracker-selective probe and C₄,C₉-BODIPY[®] fluorescent dye, respectively. As shown in Figure 3C, ROS formation in mitochondria increased in all treated cells with the highest level of damage being produced by CeO₂NPs40, followed by CeO₂NPs10, CeO₂NPs360 and CeO₂NP. Regarding cellular lipid peroxidation,

statistically significant differences were only detected for CeO₂NPs40 (Figure 3D).

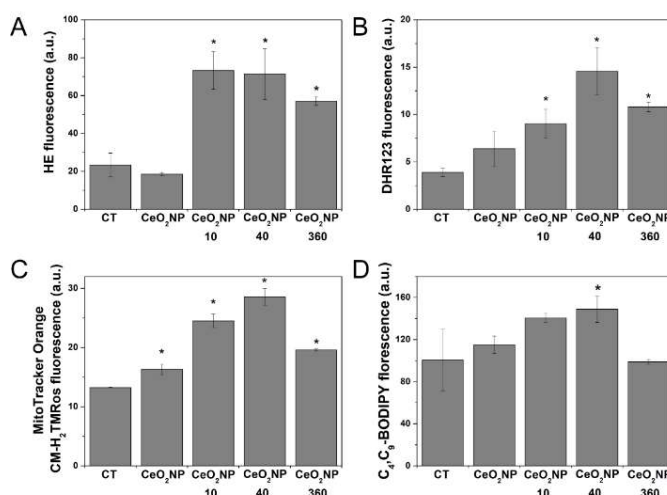


Figure 3. Effect of CeO₂NPs on intracellular superoxide anion and hydrogen peroxide levels of *C. reinhardtii* by FCM using the fluorochrome HE (A) and DHR123 (B), respectively. Alterations in mitochondrial ROS homeostasis and intracellular lipid peroxidation are also shown in (C) and (D), respectively. Statistically significant differences ($p < 0.05$) are marked by asterisks. Data are expressed as arbitrary units (a. u.).

Taking these results together, we observed a different toxicological pattern between coated and non-coated CeO₂NPs. Uncoated NP markedly damaged the algal cytoplasmic membrane, leading to limited intracellular effects. Contrarily, PVP coated CeO₂NPs caused severe intracellular damages mediated by an increase in the number of metabolically non-active cells and a strong disbalance in oxidative stress. The fact that they induced those effects without affecting directly the cytoplasmic membrane integrity may indicate that PVP-CeO₂NPs internalize, possibly by using the internalization routes described for other eukaryotic organisms⁷¹.

Internalization of CeO₂NPs

TEM was used to prove the effectiveness of the EDTA washing steps, but also, to find direct evidence of CeO₂NPs internalization (see ESI Figure S1), however, we were not able to observe the precise moment when endocytosis occurred. To investigate the internalization of CeO₂NPs from a different perspective, the distribution of cerium in the culture medium (Figure 4A and D), adsorbed to the cell wall (Figure 4B and E) and measured inside the cells (Figure 4C and F) was analyzed by ICP-MS after 12 h (Figure 4A-C) or 48 h (Figure 4D-F) of exposure. There were no differences in the cerium content in the culture medium after 12 h

of exposure (Figure 4A). However, uncoated NPs led to more cerium attached to the cell wall than PVP coated NPs (Figure B), with much less inside cells (Figure C). No differences were found among CeO₂NPs10, CeO₂NPs40 or CeO₂NPs360. Different behaviour was observed after 48 h of contact between CeO₂NPs and algal cells. CeO₂NP appeared mostly in suspension as compared to the other NPs (Figure 4D), but PVP coated NPs preferentially attached to the cell wall. Also, CeO₂NP internalized in a higher amount than the other NPs after 48 h. The differences found in the internalized NPs after 12 and 48 h of exposure (Figure 4C and 4F) might be related with the different interaction of CeO₂NPs with cytoplasmic membrane. On the one hand, PVP coated CeO₂NPs, considering that they interact with the cytoplasmic membrane without damaging it, may trigger some endocytic mechanisms, which usually take place in short periods of time, increasing the amount of internalized NPs at early stages (12 h) in comparison to uncoated NPs. On the other hand, the fact that CeO₂NP seriously damaged the cytoplasmic membrane suggests that these NPs could directly pass through membrane holes, preferentially accumulating inside the cells at higher exposure time (48 h). Although FCM analyses were performed at 24 h and the internalization studies at 48 h, the results obtained with those different approaches have given different but complementary information which can be used to link the complexity of the effects of CeO₂NPs. Furthermore, as internalization studies with environmentally relevant organisms are not yet fully studied, some processes such as NP exocytosis or, even, particle internalization blocked by saturation can not be discarded at long periods of time.

Endocytosis inhibitors and potential route of uptake

As internalization was observed for all CeO₂NPs, different endocytosis inhibitors were used in order to elucidate the uptake route involved. MDC, filipin complex, EIPA and NaN₃ were used to block the clathrin and caveolin dependent endocytosis, macropinocytosis and energy dependent endocytosis, respectively. These compounds did not cause any harmful effect at the concentrations used in this study (see ESI Figure S8). As stated above, photosynthesis was affected by all NPs (section 3.2), so algal Ch *a* fluorescence was used as a key biological parameter in order to assess the effect of inhibitors on NP internalization toxic effects. It was considered that whether an inhibitor efficiently blocked the entry of CeO₂NPs through a specific endocytic route, then the toxicity related with photosynthesis should be reduced, so that the level of Ch *a* fluorescence remained as control values. As shown in Figure 5, only the inhibitor associated with clathrin dependent endocytosis, MDC, was able to effectively block the entry of CeO₂NP, CeO₂NPs10 and CeO₂NPs360 as they were not able to induce any alteration on Ch *a* fluorescence. This was further corroborated as the level of CeO₂NPs inside cells after the MDC treatment was calculated by ICMS and supported the results shown before as MDC reduced the entry of CeO₂NP, CeO₂NP10, CeO₂NP40 and CeO₂NP360 by 17.2 %, 58.3 %, 35.9 % and 22.9 %, respectively (see ESI Figure S9), in agreement with previous work showing that inhibitors may not block the entry of NPs completely⁷².

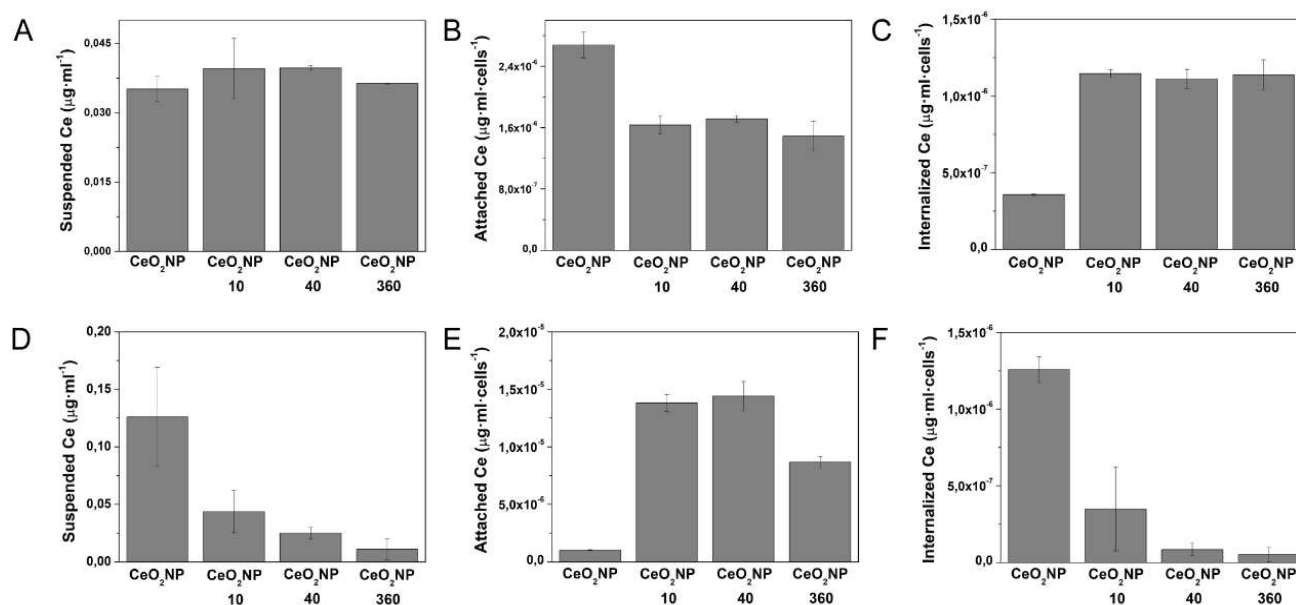


Figure 4. Analysis of the Ce content in three different compartments after 12 h (A-C) and 48 h (D-F) of exposure to CeO₂NP, CeO₂NP10, CeO₂NPs40 and CeO₂NPs360. (A and D) The Ce content as CeO₂NPs suspended in the medium. (B and E) The Ce content as CeO₂NPs adsorbed to the algal cell envelopes. (C and F) The Ce content inside cell as internalized CeO₂NPs.

The results suggested that the entry of PVP-CeO₂NPs in algal cells may be only through endocytosis, whereas CeO₂NP could enter the cells both by direct damage to the cytoplasmic membrane and by endocytosis processes as has been demonstrated with these internalization experiments. The results found here also suggest that CeO₂NPs uptake in *C. reinhardtii* may be mediated by clathrin-dependant endocytosis.

Effect of CeO₂NPs on transcription of the *CHC1* gene

As clathrin-dependent endocytosis was revealed as the main endocytic route of CeO₂NPs internalization, RT-qPCR was used to determine changes in the expression of *CHC1*; a gene in *C. reinhardtii* thought to be involved in clathrin-mediated endocytosis⁵⁹. It is worth noting that the present work is the first aiming at attempting a genetic approach on endocytosis in this organism as no experimental evidence on the role of this gene is available up to date. Though little is known about endocytosis in *C. reinhardtii*, clathrin-coated vesicles have been purified from both wild type and a wall-less mutant cells⁷³, supporting genetic evidence of clathrin-mediated endocytosis in this organism. Figure 6 shows the effect of CeO₂NPs on expression of this gene. At a short exposure time of 1 h, *CHC1* expression was upregulated by 31.7 %, 32.7 %, 33.2 % and 69.1 % for CeO₂NP, CeO₂NPs10, CeO₂NPs40 and CeO₂NPs360, respectively. However, there were no statistical differences at longer exposure time (4 h; ESI Figure S10), indicating that NP internalization process starts on first contact between algal cells and NPs, particularly for PVP-coated CeO₂NPs with increased internalization after only 12 h of exposure (Figure 4C).

Discussion

Due to their unique properties, CeO₂NPs have several interesting current and potential future applications that make them one of the most promising nanomaterials. However, their widespread use may increase their presence in the environment. Based on the results presented here, the actual highest predicted environmental concentration did not cause any adverse effect on *C. reinhardtii* nor in terms of microalgal growth inhibition or in the analyzed physiological parameters. Therefore, the environmental risk of CeO₂NPs may be low according to the available data, although it should be emphasized that chronic exposure even at low concentration may cause adverse effects and merits further studies^{40, 74}. However, to define the actual hazard of CeO₂NPs, it will be necessary to determine the real concentration of these nanoparticles in the environment or to create probabilistic models which improve the current knowledge and to test those concentrations in a battery of environmentally relevant organisms.

From a mechanistic point of view, we have found evidences that CeO₂NPs may be internalized by algae cells and provoke a strong toxic response in the green alga *C. reinhardtii*, mediated by an increase of intracellular ROS or by direct damage to the cytoplasmic membrane. Several studies have previously reported that CeO₂NPs are toxic to algae and other aquatic organisms^{26, 27, 29}. Mechanistic studies, however, are scarce. Here, a combined approach of cellular, physiological and genetic analyses has provided novel insights into toxicological and internalization mechanisms of coated and uncoated CeO₂NPs in a model aquatic organism. As far as we know, this is also the first time that internalization and toxic mechanisms could be related and associated to different types of CeO₂NPs. However, it is worth noting that some non-internalized NPs may also have an impact on the overall toxicity. They may affect the cell envelopes and trigger an intracellular toxic response as previously shown for uncoated CeO₂NPs by means of the interference with the nutrient transport function of the membrane⁷⁵ or through ROS generation and oxidative stress induction^{28, 76}.

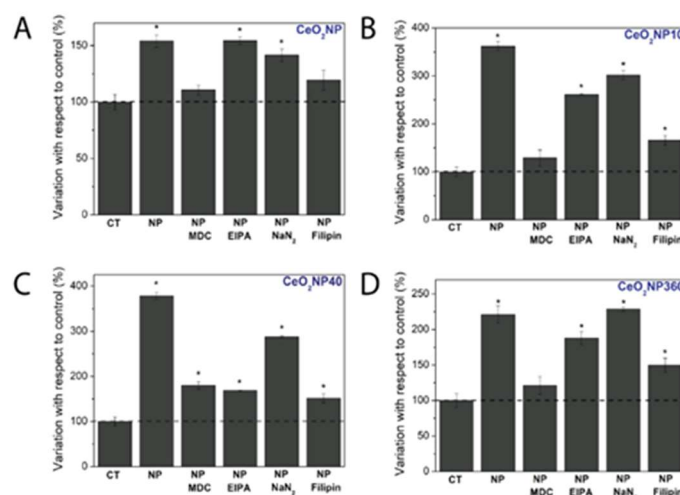


Figure 5. Analysis of the effect of CeO₂NPs (CeO₂NP, CeO₂NPs10, CeO₂NPs40 and CeO₂NPs360) and inhibitors (MDC, EIPA, NaN₃ and filipin complex) on Ch *a* fluorescence of *C. reinhardtii*. CT: control. Statistically significant differences ($p < 0.05$) are marked by asterisks.

PVP-CeO₂NPs exerted toxicity by means of a different toxicological mechanism than uncoated CeO₂NP. According to the results obtained in this work, cellular membrane integrity was only compromised by the uncoated NP, CeO₂NP, (Figure 2A), indicating that the initial effect of CeO₂NP takes place by interaction with the algal cytoplasmic membrane. Conversely, PVP-coated NPs did not affect the cytoplasmic membrane but induced a strong increase in intracellular ROS (both O₂^{•-} and H₂O₂; Figure 3A-B), which led to an increase in mitochondrial ROS formation (Figure 3C) and in the

level of intracellular lipid peroxidation for the specific case of CeO₂NPs40. There was no significant increase in the intracellular ROS of algal cells exposed to uncoated CeO₂NP, demonstrating that the direct physical damage to the cellular membrane was the main mechanism explaining the observed toxicity for this NP. Nowadays, CeO₂NPs are surrounded by controversy regarding their biological effects; many authors revealed their reactivity and antioxidant properties, which make them useful for biomedical applications^{15, 77, 78}. However, other studies showed that these NPs could also behave as toxic compounds to a variety of cell lines and organisms^{29, 79, 80}. According to the results reported here, the biological effects of CeO₂NPs should be revisited considering the effect of polymeric coatings. Recently, the percentage of surface Ce³⁺ of CeO₂NPs has been revealed as a key factor which drives the toxicity of uncoated CeO₂NPs²⁸. However, this property may be of lower importance if CeO₂NPs are covered with capping agents as the uncoated CeO₂NPs and coated CeO₂NP10 used in this study exhibited similar % of surface Ce³⁺, but they displayed completely different toxicological mechanisms. Moreover, it has been shown that the reactivity of CeO₂NPs may reduce while increasing the thickness of different types of polymeric coatings¹⁸, therefore the type and thickness of polymeric coating is an important factor in particle reactivity. The results showed here support this hypothesis as CeO₂NPs360 with a coating of 360 kDa induced a lower extent of biological effects in comparison with the other coated particles with 10 kDa and 40 kDa PVP.

Our results showed that the PVP coating of CeO₂NPs influence the internalization kinetics. After 12 h, internalization was found mostly for PVP-coated NPs while after 48 h the highest level of Ce was found for CeO₂NP. This suggests that as membrane damage increases with time, CeO₂NP may pass through more easily and accumulate inside cells (Figure 4F), explaining their presence in higher amount at later exposure times. PVP-coated CeO₂NPs also interacted with the cellular membrane, but without damaging it and being adsorbed at higher amount to the cell envelopes after 48 h of exposure (Figure 4E). The reasonable explanation of these findings is that PVP coating protected cells from the direct contact with the NP core, but at the same time promoted NP internalization during the early stages of exposure (Figure 4C and Figure 6). The coating itself may enhance the interaction with cells by attaching to certain specific groups at the cytoplasmic membrane. In the same way as bare NPs are surrounded by different biomolecules, forming the so-called protein corona or eco-corona; PVP-coated NPs by enhancing the interaction with cellular envelopes and triggering endocytic processes⁸¹⁻⁸⁶ could behave similarly.

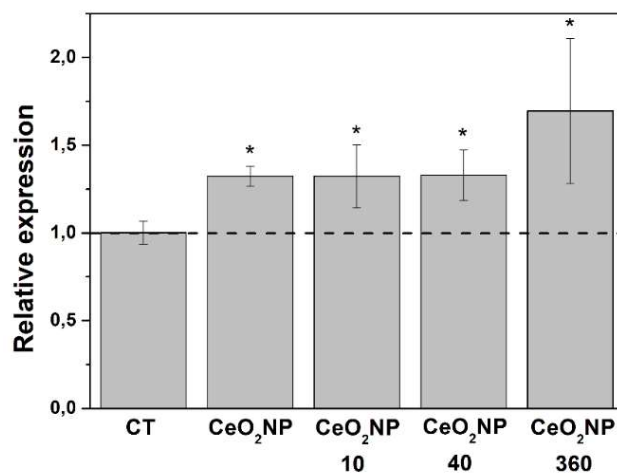


Figure 6. Effect of CeO₂NPs on expression of *CHC1* gene after 1 h of exposure. Data is represented as relative expression of the genes with respect to the unexposed control (Tukey's HSD, $p < 0.05$). Control values were set to 1 for easy comparison. Statistically significant differences ($p < 0.05$) are marked by asterisks.

NP internalization has been recently observed in *C. reinhardtii* for QdTe/CdS Quantum Dots⁸⁷, PAMAM-dendrimers⁸⁸ and for Ag⁴¹, CeO₂⁴⁰ and CuO⁴² NPs. However, works studying the mechanism of entry in cells are scarce. Many works have studied the machinery related to endocytosis in higher plants^{89, 90}. However, little is known about this process in algae. It has been shown that there exist several routes of endocytosis in eukaryotic organisms⁷¹ that explain the internalization of nanomaterials in several environmentally relevant organisms^{58, 91-93}. Wang et al.⁹¹ showed that CdTe Quantum Dots could enter the freshwater alga *Ochromonas danica* directly through micropinocytosis. Moreover, Hoepflinger et al. reported that clathrin-dependent pathway played an important role in the endocytosis process in a multicellular green alga (*Chara australis*)⁹⁴. The genomic mapping of *C. reinhardtii* together with some experimental studies have revealed that this microalgae possesses a clathrin-mediated endocytosis pathway^{59, 73, 95} and also that ceria NPs can be internalized⁴⁰. In the present study, we have shown that clathrin-dependent endocytosis is the main route of CeO₂NPs entry into the cells of *C. reinhardtii* as MDC (molecule that stabilizes clathrin-coated pits) blocked the entry of all CeO₂NPs, avoiding their toxic effects related with the photosynthetic apparatus. However, it is worth noting that, in general terms, the internalization of NPs may only occur under certain circumstances. First, particle size is an issue. It has been shown that the cell wall constitutes the first barrier with a pore diameter in the 5-20 nm range⁹⁶, so internalization of larger or agglomerated particles seems rather improbable, unless they enter (i) via the apical zone where the presence of flagella causes an absence of cell wall⁷⁹ or (ii) during the reproduction

period when the newly synthesized cell walls are more facile to penetrate⁹⁷. Second, as PVP-CeO₂NPs were able to solely internalize through endocytosis mechanisms, the use of capping agents might also play an important role, enhancing and triggering the endocytic system after interacting with the cytoplasmic membrane.

Several authors have previously shown that the dissolution of CeO₂NPs may be enhanced at the bio-nano interface and promote the entry of Ce³⁺ ions more easily^{98,99}. Ma et al⁹⁹ showed that the physicochemical interaction between the NPs and root exudates at the nano-bio interface is the required condition for the transformation of CeO₂NPs in plant systems. The plant exudates (including organic acids) are known to alter the surrounding environment, impact the rhizobial community, support beneficial symbioses, alter the chemical and physical properties of the soil, among others¹⁰⁰. Different studies have shown that exudates could also interact with nanomaterials, promoting NP dissolution¹⁰¹⁻¹⁰³. This seems unlikely in the case with *C. reinhardtii* as the release of exudates and organic acids are quite more limited in algal cells in comparison with the plethora of compounds released by plants^{104,105}. Moreover, the specific physicochemical characteristics of NPs are of crucial importance for determining the reactivity of CeO₂NPs. Xie et al⁹⁸ used rod-CeO₂NPs which are NPs with higher concentration of surface defects, and, thus, higher reactivity rates in comparison with other morphologies^{106,107}. Here, the used CeO₂NPs were spheres coated with PVP, so the surface reactivity may be limited due to the shielding effect of the coating.

Despite the limited available information about endocytosis in plant cells in comparison with the existing grounded-knowledge for animal cells, different works have highlighted the importance of this process as a crucial mechanism by which plants cells internalize extracellular and plasma membrane material^{108,109}. Several authors have also underlined its role in the well-functioning of the cells, specifically how clathrin dependent endocytosis is involved in key physiological processes^{110,111}. Here, using *C. reinhardtii* as model of study, we have found that CeO₂NPs generated an overexpression of *CHC1*, gene involved in the clathrin-mediated endocytosis. If this phenomenon implies a biological significance is unknown since cerium is not an essential nutrient for microalgae. Besides, whether nanoparticle internalization is performed to alleviate the impact of CeO₂NPs in the cellular envelopes or because they obtain an unknown benefit or whether they are mistakenly introduced has to be deeply studied in the future.

As far as we know, based on inhibitors and gene expression analysis, this is the first time that it is shown

that clathrin-dependent pathway is the main route of entry of nanoparticles into *C. reinhardtii* cells. Further research is still needed for determining the effect of other coatings in CeO₂NPs uptake and also, the optimal PVP-chain length that could favour the internalization of NPs. More research is still needed to fully understand the NP internalization (in terms of genes involved and timing of the process) by endocytosis in the green alga.

Conclusions

In this work, we have reported a thorough study on the toxicological effects of uncoated and PVP-coated CeO₂NPs to *C. reinhardtii*. Monodispersed NPs of cerium oxide and PVP-coated cerium oxide were synthesized and physicochemically characterized in the exposure media. Overall, we conclude that the risks to *C. reinhardtii* posed by the uncoated and coated CeO₂NPs used here at the predicted environmental concentrations are low, although it should be emphasized that chronic exposure even at low concentration may cause adverse effects and merits further studies. From a mechanistic point of view using higher concentrations, the toxicity of the bare CeO₂NP took place by damage to cytoplasmic membrane, which eventually caused a decrease in metabolic activity. PVP-coated NPs exerted their toxicity by intracellular ROS formation without direct damage to the cell membrane. Different degrees of cell damage were found depending on PVP chain length, being CeO₂NPs40 the most toxic NP, followed by CeO₂NPs10. Moreover, internalization evidences were found for all NPs, but, after 48 h of exposure, CeO₂NP was internalized in higher proportion than PVP-coated CeO₂NPs, which predominantly appeared attached to the algal envelopes. The studies performed using endocytosis inhibitors indicated that clathrin-dependent endocytosis was the main pathway for NP entry. As internalization is a complex process with little available information for environmental organisms such as algae, different qualitatively and quantitatively techniques as well as diverse experimental time scales have been performed to better understand the interaction between CeO₂NPs and *C. reinhardtii*. The results shown here highlight the importance of assessing the toxicity of CeO₂NPs as they are intended to be used and found in the environment due to the toxicological mechanism could be significantly different, depending on NP coating. As discussed above, the surface coating totally changes the interaction of nanomaterials with the environment, so there is still a long way to get a complete picture of the effects of coated nanomaterials in living organisms. Nonetheless, the information presented here will be useful for shedding light regarding the contradictory effects of CeO₂NPs that

have been reported in the scientific literature and for the synthesis of safer-by-design nanomaterials.

Acknowledgement

This research was supported by CTM2013-45775-C2-1,2-R and CTM2016-74927-C2-1,2-R grants from MINECO. NanoMILE (Grant Agreement no 310451 to EVJ & SMB) and the Endeavour Scholarship Scheme (Group B) (to SMB).

References

1. R. A. Sperling and W. Parak, Surface modification, functionalization and bioconjugation of colloidal inorganic nanoparticles, *Philosophical Transactions of the Royal Society of London A: Mathematical, Physical and Engineering Sciences*, 2010, **368**, 1333-1383.
2. Y. A. Wang, J. J. Li, H. Chen and X. Peng, Stabilization of inorganic nanocrystals by organic dendrons, *Journal of the American Chemical Society*, 2002, **124**, 2293-2298.
3. R. B. Grubbs, Roles of polymer ligands in nanoparticle stabilization, *Polymer Reviews*, 2007, **47**, 197-215.
4. M. Tsuji, N. Miyamae, S. Lim, K. Kimura, X. Zhang, S. Hikino and M. Nishio, Crystal structures and growth mechanisms of Au@Ag core-shell nanoparticles prepared by the microwave-polyol method, *Crystal growth & design*, 2006, **6**, 1801-1807.
5. A. Guerrero-Martínez, J. Pérez-Juste and L. M. Liz-Marzán, Recent progress on silica coating of nanoparticles and related nanomaterials, *Advanced materials*, 2010, **22**, 1182-1195.
6. C. Roma-Rodrigues, A. Heuer-Jungemann, A. R. Fernandes, A. G. Kanaras and P. V. Baptista, Peptide-coated gold nanoparticles for modulation of angiogenesis in vivo, *International Journal of Nanomedicine*, 2016, **11**, 2633.
7. S. Uthaman, S. J. Lee, K. Cherukula, C.-S. Cho and I.-K. Park, Polysaccharide-coated magnetic nanoparticles for imaging and gene therapy, *BioMed research international*, 2015, **2015**.
8. X. Li, J. J. Lenhart and H. W. Walker, Aggregation kinetics and dissolution of coated silver nanoparticles, *Langmuir : the ACS journal of surfaces and colloids*, 2012, **28**, 1095-1104.
9. N. T. Thanh and L. A. Green, Functionalisation of nanoparticles for biomedical applications, *Nano Today*, 2010, **5**, 213-230.
10. T. X. Sayle, M. Molinari, S. Das, U. M. Bhatta, G. Möbus, S. C. Parker, S. Seal and D. C. Sayle, Environment-mediated structure, surface redox activity and reactivity of ceria nanoparticles, *Nanoscale*, 2013, **5**, 6063-6073.
11. K. Reed, A. Cormack, A. Kulkarni, M. Mayton, D. Sayle, F. Klaessig and B. Stadler, Exploring the properties and applications of nanoceria: is there still plenty of room at the bottom?, *Environmental Science: Nano*, 2014, **1**, 390-405.
12. P. Chaturvedi, D. Vanegas, M. Taguchi, S. Burrs, P. Sharma and E. McLamore, A nanoceria-platinum-graphene nanocomposite for electrochemical biosensing, *Biosensors and Bioelectronics*, 2014, **58**, 179-185.
13. J. Colon, L. Herrera, J. Smith, S. Patil, C. Komanski, P. Kupelian, S. Seal, D. W. Jenkins and C. H. Baker, Protection from radiation-induced pneumonitis using cerium oxide nanoparticles, *Nanomedicine: Nanotechnology, Biology and Medicine*, 2009, **5**, 225-231.
14. R. Zandi Zand, K. Verbeken and A. Adriaens, Evaluation of the corrosion inhibition performance of silane coatings filled with cerium salt-activated nanoparticles on hot-dip galvanized steel substrates, *International Journal of Electrochemical Science*, 2013, **8**, 4927-4940.
15. G. Pulido-Reyes, S. Das, F. Leganés, S. Silva, S. Wu, W. Self, F. Fernández-Piñas, R. Rosal and S. Seal, Hypochlorite scavenging activity of cerium oxide nanoparticles, *RSC Advances*, 2016, **6**, 62911-62915.
16. C. Xu, Z. Liu, L. Wu, J. Ren and X. Qu, Nucleoside Triphosphates as Promoters to Enhance Nanoceria Enzyme-like Activity and for Single-Nucleotide Polymorphism Typing, *Advanced Functional Materials*, 2014, **24**, 1624-1630.
17. C. Xu and X. Qu, Cerium oxide nanoparticle: a remarkably versatile rare earth nanomaterial for biological applications, *NPG Asia Materials*, 2014, **6**, e90.
18. S. S. Lee, W. Song, M. Cho, H. L. Puppala, P. Nguyen, H. Zhu, L. Segatori and V. L. Colvin, Antioxidant properties of cerium oxide nanocrystals as a function of nanocrystal diameter and surface coating, *ACS nano*, 2013, **7**, 9693-9703.
19. L. Qi, A. Sehgal, J.-C. Castaing, J.-P. Chapel, J. Fresnais, J.-F. Berret and F. Cousin, Redispersible hybrid nanopowders: cerium oxide nanoparticle complexes with phosphonated-PEG oligomers, *ACS nano*, 2008, **2**, 879-888.
20. A. Asati, S. Santra, C. Kaittanis, S. Nath and J. M. Perez, Oxidase-like activity of polymer-coated cerium oxide nanoparticles, *Angewandte Chemie*, 2009, **48**, 2308-2312.
21. A. S. Karakoti, S. Singh, A. Kumar, M. Malinska, S. V. Kuchibhatla, K. Wozniak, W. T. Self and S. Seal, PEGylated nanoceria as radical scavenger with tunable redox chemistry, *Journal of the American Chemical Society*, 2009, **131**, 14144-14145.
22. S. Briffa, I. Lynch, V. Trouillet, M. Bruns, D. Hapiuk, J. Liu, R. Palmer and E. Valsami-Jones, Development of scalable and versatile nanomaterial libraries for nanosafety studies: polyvinylpyrrolidone (PVP) capped metal oxide nanoparticles, *RSC Advances*, 2017, **7**, 3894-3906.
23. Z. Wu, J. Zhang, R. E. Benfield, Y. Ding, D. Grandjean, Z. Zhang and X. Ju, Structure and chemical transformation in cerium oxide nanoparticles coated by surfactant cetyltrimethylammonium bromide (CTAB): an X-ray absorption spectroscopic study, *The Journal of Physical Chemistry B*, 2002, **106**, 4569-4577.
24. M. Hijaz, S. Das, I. Mert, A. Gupta, Z. Al-Wahab, C. Tebbe, S. Dar, J. Chhina, S. Giri and A. Munkarah, Folic acid tagged nanoceria as a novel therapeutic agent in ovarian cancer, *BMC cancer*, 2016, **16**, 220.

25. S. Das, J. M. Dowding, K. E. Klump, J. F. McGinnis, W. Self and S. Seal, Cerium oxide nanoparticles: applications and prospects in nanomedicine, *Nanomedicine (London, England)*, 2013, **8**, 1483-1508.
26. I. Rodea-Palomares, K. Boltos, F. Fernandez-Pinas, F. Leganes, E. Garcia-Calvo, J. Santiago and R. Rosal, Physicochemical characterization and ecotoxicological assessment of CeO₂ nanoparticles using two aquatic microorganisms, *Toxicological sciences : an official journal of the Society of Toxicology*, 2011, **119**, 135-145.
27. E. Artells, J. Issartel, M. Auffan, D. Borschneck, A. Thill, M. Tella, L. Brousset, J. Rose, J.-Y. Bottero and A. Thiéry, Exposure to cerium dioxide nanoparticles differently affect swimming performance and survival in two daphnid species, *PLoS one*, 2013, **8**, e71260.
28. G. Pulido-Reyes, I. Rodea-Palomares, S. Das, T. S. Sakthivel, F. Leganes, R. Rosal, S. Seal and F. Fernández-Piñas, Untangling the biological effects of cerium oxide nanoparticles: the role of surface valence states, *Scientific Reports*, 2015, **5**, 15613.
29. N. Manier, A. Bado-Nilles, P. Delalain, O. Aguerre-Chariol and P. Pandard, Ecotoxicity of non-aged and aged CeO₂ nanomaterials towards freshwater microalgae, *Environmental pollution*, 2013, **180**, 63-70.
30. S. Mittal and A. K. Pandey, Cerium oxide nanoparticles induced toxicity in human lung cells: role of ROS mediated DNA damage and apoptosis, *BioMed research international*, 2014, **2014**.
31. H. Zhang, X. He, Z. Zhang, P. Zhang, Y. Li, Y. Ma, Y. Kuang, Y. Zhao and Z. Chai, Nano-CeO₂ exhibits adverse effects at environmental relevant concentrations, *Environmental science & technology*, 2011, **45**, 3725-3730.
32. F. Caputo, M. De Nicola, A. Sienkiewicz, A. Giovanetti, I. Bejarano, S. Licoccia, E. Traversa and L. Ghibelli, Cerium oxide nanoparticles, combining antioxidant and UV shielding properties, prevent UV-induced cell damage and mutagenesis, *Nanoscale*, 2015, **7**, 15643-15656.
33. K. Chaudhury, K. N. Babu, A. K. Singh, S. Das, A. Kumar and S. Seal, Mitigation of endometriosis using regenerative cerium oxide nanoparticles, *Nanomedicine : nanotechnology, biology, and medicine*, 2013, **9**, 439-448.
34. E. G. Heckert, A. S. Karakoti, S. Seal and W. T. Self, The role of cerium redox state in the SOD mimetic activity of nanoceria, *Biomaterials*, 2008, **29**, 2705-2709.
35. T. Pirmohamed, J. M. Dowding, S. Singh, B. Wasserman, E. Heckert, A. S. Karakoti, J. E. King, S. Seal and W. T. Self, Nanoceria exhibit redox state-dependent catalase mimetic activity, *Chemical communications*, 2010, **46**, 2736-2738.
36. X.-Y. Deng, J. Cheng, X.-L. Hu, L. Wang, D. Li and K. Gao, Biological effects of TiO₂ and CeO₂ nanoparticles on the growth, photosynthetic activity, and cellular components of a marine diatom *Phaeodactylum tricorutum*, *Science of the Total Environment*, 2017, **575**, 87-96.
37. Y. H. Leung, M. M. Yung, A. M. Ng, A. P. Ma, S. W. Wong, C. M. Chan, Y. H. Ng, A. B. Djurišić, M. Guo and M. T. Wong, Toxicity of CeO₂ nanoparticles—The effect of nanoparticle properties, *Journal of Photochemistry and Photobiology B: Biology*, 2015, **145**, 48-59.
38. E.-J. Park, J. Choi, Y.-K. Park and K. Park, Oxidative stress induced by cerium oxide nanoparticles in cultured BEAS-2B cells, *Toxicology*, 2008, **245**, 90-100.
39. L. A. K. née Röhder, T. Brandt, L. Sigg and R. Behra, Uptake and effects of cerium (III) and cerium oxide nanoparticles to *Chlamydomonas reinhardtii*, *Aquatic Toxicology*, 2018, **197**, 41-46.
40. N. S. Taylor, R. Merrifield, T. D. Williams, J. K. Chipman, J. R. Lead and M. R. Viant, Molecular toxicity of cerium oxide nanoparticles to the freshwater alga *Chlamydomonas reinhardtii* is associated with supra-environmental exposure concentrations, *Nanotoxicology*, 2015, DOI: 10.3109/17435390.2014.1002868, 1-10.
41. S. Wang, J. Lv, J. Ma and S. Zhang, Cellular internalization and intracellular biotransformation of silver nanoparticles in *Chlamydomonas reinhardtii*, *Nanotoxicology*, 2016, **10**, 1129-1135.
42. F. Perreault, A. Oukarroum, S. P. Melegari, W. G. Matias and R. Popovic, Polymer coating of copper oxide nanoparticles increases nanoparticles uptake and toxicity in the green alga *Chlamydomonas reinhardtii*, *Chemosphere*, 2012, **87**, 1388-1394.
43. T. Marie, A. Mélanie, B. Lenka, I. Julien, K. Isabelle, P. Christine, M. Elise, S. Catherine, A. Bernard and A. Ester, Transfer, transformation, and impacts of ceria nanomaterials in aquatic mesocosms simulating a pond ecosystem, *Environmental science & technology*, 2014, **48**, 9004-9013.
44. A. Bour, F. Mouchet, S. Cadarsi, J. Silvestre, D. Baqué, L. Gauthier and E. Pinelli, CeO₂ nanoparticle fate in environmental conditions and toxicity on a freshwater predator species: a microcosm study, *Environmental Science and Pollution Research*, 2017, **24**, 17081-17089.
45. A. Booth, T. Størseth, D. Altin, A. Fornara, A. Ahniyaz, H. Jungnickel, P. Laux, A. Luch and L. Sørensen, Freshwater dispersion stability of PAA-stabilised cerium oxide nanoparticles and toxicity towards *Pseudokirchneriella subcapitata*, *Science of the Total Environment*, 2015, **505**, 596-605.
46. J.-D. Cafun, K. O. Kvashnina, E. Casals, V. F. Puentes and P. Glatzel, Absence of Ce³⁺ sites in chemically active colloidal ceria nanoparticles, *ACS Nano*, 2013, **7**, 10726-10732.
47. S. Deshpande, S. Patil, S. V. Kuchibhatla and S. Seal, Size dependency variation in lattice parameter and valency states in nanocrystalline cerium oxide, *Applied Physics Letters*, 2005, **87**, 133113.
48. S. Gonzalo, V. Llana, G. Pulido-Reyes, F. Fernandez-Pinas, J. C. Bonzongo, F. Leganes, R. Rosal, E. Garcia-Calvo and I. Rodea-Palomares, A colloidal singularity reveals the crucial role of colloidal stability for nanomaterials in-vitro toxicity testing: nZVI-microalgae colloidal system as a case study, *PLoS one*, 2014, **9**, e109645.
49. D. S. Gorman and R. P. Levine, Cytochrome f and plastocyanin: their sequence in the photosynthetic

- electron transport chain of *Chlamydomonas reinhardtii*, *Proceedings of the National Academy of Sciences of the United States of America*, 1965, **54**, 1665-1669.
50. O. T. No, 201: Freshwater alga and cyanobacteria, growth inhibition test, *OECD guidelines for the testing of chemicals, section*, 2011, **2**.
 51. J. Dorsey, C. M. Yentsch, S. Mayo and C. McKenna, Rapid analytical technique for the assessment of cell metabolic activity in marine microalgae, *Cytometry: The Journal of the International Society for Analytical Cytology*, 1989, **10**, 622-628.
 52. F. J. Jochem, Dark survival strategies in marine phytoplankton assessed by cytometric measurement of metabolic activity with fluorescein diacetate, *Marine biology*, 1999, **135**, 721-728.
 53. M. González-Pleiter, C. Rioboo, M. Reguera, I. Abreu, F. Leganés, Á. Cid and F. Fernández-Piñas, Calcium mediates the cellular response of *Chlamydomonas reinhardtii* to the emerging aquatic pollutant Triclosan, *Aquatic toxicology*, 2017, **186**, 50-66.
 54. F. Spedding, J. Powell and E. J. Wheelwright, The stability of the rare earth complexes with N-hydroxyethylethylenediaminetriacetic acid, *Journal of the American Chemical Society*, 1956, **78**, 34-37.
 55. P. Schlossmacher, D. O. Klenov, B. Freitag, S. von Harrach and A. Steinbach, Nanoscale chemical compositional analysis with an innovative S/TEM-EDX system, *Microscopy and analysis*, 2010, **5**.
 56. S. Vranic, N. Boggetto, V. Contremoulins, S. Mornet, N. Reinhardt, F. Marano, A. Baeza-Squiban and S. Boland, Deciphering the mechanisms of cellular uptake of engineered nanoparticles by accurate evaluation of internalization using imaging flow cytometry, *Particle and fibre toxicology*, 2013, **10**, 2.
 57. J. Rejman, A. Bragonzi and M. Conese, Role of clathrin-and caveolae-mediated endocytosis in gene transfer mediated by lipo-and polyplexes, *Molecular Therapy*, 2005, **12**, 468-474.
 58. Z. Wang, J. Li, J. Zhao and B. Xing, Toxicity and internalization of CuO nanoparticles to prokaryotic alga *Microcystis aeruginosa* as affected by dissolved organic matter, *Environ Sci Technol*, 2011, **45**, 6032-6040.
 59. S. S. Merchant, S. E. Prochnik, O. Vallon, E. H. Harris, S. J. Karpowicz, G. B. Witman, A. Terry, A. Salamov, L. K. Fritz-Laylin and L. Maréchal-Drouard, The *Chlamydomonas* genome reveals the evolution of key animal and plant functions, *Science*, 2007, **318**, 245-250.
 60. K. J. Livak and T. D. Schmittgen, Analysis of relative gene expression data using real-time quantitative PCR and the 2- $\Delta\Delta$ CT method, *methods*, 2001, **25**, 402-408.
 61. H.-X. Mai, L.-D. Sun, Y.-W. Zhang, R. Si, W. Feng, H.-P. Zhang, H.-C. Liu and C.-H. Yan, Shape-selective synthesis and oxygen storage behavior of ceria nanopolyhedra, nanorods, and nanocubes, *The Journal of Physical Chemistry B*, 2005, **109**, 24380-24385.
 62. X. Liu, K. Zhou, L. Wang, B. Wang and Y. Li, Oxygen vacancy clusters promoting reducibility and activity of ceria nanorods, *Journal of the American Chemical Society*, 2009, **131**, 3140-3141.
 63. D. Jiang, W. Wang, L. Zhang, Y. Zheng and Z. Wang, Insights into the surface-defect dependence of photoreactivity over CeO₂ nanocrystals with well-defined crystal facets, *ACS Catalysis*, 2015, **5**, 4851-4858.
 64. S. Das, S. Singh, J. M. Dowding, S. Oommen, A. Kumar, T. X. Sayle, S. Saraf, C. R. Patra, N. E. Vlahakis and D. C. Sayle, The induction of angiogenesis by cerium oxide nanoparticles through the modulation of oxygen in intracellular environments, *Biomaterials*, 2012, **33**, 7746-7755.
 65. D. Franqueira, M. Orosa, E. Torres, C. Herrero and A. Cid, Potential use of flow cytometry in toxicity studies with microalgae, *Science of the total environment*, 2000, **247**, 119-126.
 66. P. Eullaffroy and G. Vernet, The F684/F735 chlorophyll fluorescence ratio: a potential tool for rapid detection and determination of herbicide phytotoxicity in algae, *Water research*, 2003, **37**, 1983-1990.
 67. W. Schwarz, *PVP: a critical review of the kinetics and toxicology of polyvinylpyrrolidone (povidone)*, CRC Press, 1990.
 68. I. C. Mori, C. R. Arias-Barreiro, A. Koutsaftis, A. Ogo, T. Kawano, K. Yoshizuka, S. H. Inayat-Hussain and I. Aoyama, Toxicity of tetramethylammonium hydroxide to aquatic organisms and its synergistic action with potassium iodide, *Chemosphere*, 2015, **120**, 299-304.
 69. N. J. O'Brien and E. J. Cummins, A risk assessment framework for assessing metallic nanomaterials of environmental concern: aquatic exposure and behavior, *Risk Analysis: An International Journal*, 2011, **31**, 706-726.
 70. N. von Moos and V. I. Slaveykova, Oxidative stress induced by inorganic nanoparticles in bacteria and aquatic microalgae--state of the art and knowledge gaps, *Nanotoxicology*, 2014, **8**, 605-630.
 71. M. Zhu, G. Nie, H. Meng, T. Xia, A. Nel and Y. Zhao, Physicochemical properties determine nanomaterial cellular uptake, transport, and fate, *Acc Chem Res*, 2013, **46**, 622-631.
 72. F. R. Khan, S. K. Misra, N. R. Bury, B. D. Smith, P. S. Rainbow, S. N. Luoma and E. Valsami-Jones, Inhibition of potential uptake pathways for silver nanoparticles in the estuarine snail *Peringia ulvae*, *Nanotoxicology*, 2015, **9**, 493-501.
 73. G. M. DENNING and A. B. FULTON, Purification and characterization of clathrin-coated vesicles from *Chlamydomonas*, *The Journal of protozoology*, 1989, **36**, 334-340.
 74. Y. Dogra, K. P. Arkill, C. Elgy, B. Stolpe, J. Lead, E. Valsami-Jones, C. R. Tyler and T. S. Galloway, Cerium oxide nanoparticles induce oxidative stress in the sediment-dwelling amphipod *Corophium volutator*, *Nanotoxicology*, 2016, **10**, 480-487.
 75. O. Zeyons, A. Thill, F. Chauvat, N. Menguy, C. Cassier-Chauvat, C. Oréar, J. Daraspe, M. Auffan, J. Rose and O. Spalla, Direct and indirect CeO₂ nanoparticles toxicity for *Escherichia coli* and *Synechocystis*, *Nanotoxicology*, 2009, **3**, 284-295.
 76. I. Rodea-Palomares, S. Gonzalo, J. Santiago-Morales, F. Leganés, E. García-Calvo, R. Rosal and F. Fernández-Piñas, An insight into the mechanisms of nanoceria toxicity in aquatic photosynthetic organisms, *Aquatic toxicology*, 2012, **122**, 133-143.

77. A. Dhall and W. Self, Cerium Oxide Nanoparticles: A Brief Review of Their Synthesis Methods and Biomedical Applications, *Antioxidants (Basel, Switzerland)*, 2018, **7**.
78. F. Corsi, F. Caputo, E. Traversa and L. Ghibelli, Not only redox: the multifaceted activity of cerium oxide nanoparticles in cancer prevention and therapy, *Frontiers in Oncology*, 2018, **8**, 309.
79. M. Sendra, P. Yeste, I. Moreno-Garrido, J. Gatica and J. Blasco, CeO₂ NPs, toxic or protective to phytoplankton? Charge of nanoparticles and cell wall as factors which cause changes in cell complexity, *Science of The Total Environment*, 2017, **590**, 304-315.
80. C. Gagnon, A. Bruneau, P. Turcotte, M. Pilote and F. Gagne, Fate of Cerium Oxide Nanoparticles in Natural Waters and Immunotoxicity in Exposed Rainbow Trout, *Journal of Nanomedicine & Nanotechnology*, 2018, **9**.
81. J. Mazzolini, R. J. Weber, H.-S. Chen, A. Khan, E. Guggenheim, R. K. Shaw, J. K. Chipman, M. R. Viant and J. Z. Rappoport, Protein corona modulates uptake and toxicity of nanoceria via clathrin-mediated endocytosis, *The Biological Bulletin*, 2016, **231**, 40-60.
82. S. Ritz, S. Schöttler, N. Kotman, G. Baier, A. Musyanovych, J. r. Kuharev, K. Landfester, H. r. Schild, O. Jahn and S. Tenzer, Protein corona of nanoparticles: distinct proteins regulate the cellular uptake, *Biomacromolecules*, 2015, **16**, 1311-1321.
83. F. Nasser and I. Lynch, Secreted protein eco-corona mediates uptake and impacts of polystyrene nanoparticles on *Daphnia magna*, *Journal of proteomics*, 2016, **137**, 45-51.
84. S. M. Briffa, F. Nasser, E. Valsami-Jones and I. Lynch, Uptake and Impacts of Polyvinylpyrrolidone (PVP) Capped Metal Oxide nanoparticles on *Daphnia magna*: role of core composition and acquired corona, *Environmental Science: Nano*, 2018.
85. L. Canesi, T. Balbi, R. Fabbri, A. Salis, G. Damonte, M. Volland and J. Blasco, Biomolecular coronas in invertebrate species: Implications in the environmental impact of nanoparticles, *NanoImpact*, 2017, **8**, 89-98.
86. G. Pulido-Reyes, F. Leganes, F. Fernández-Piñas and R. Rosal, Bio-nano interface and environment: A critical review, *Environmental toxicology and chemistry*, 2017, **36**, 3181-3193.
87. R. F. Domingos, D. F. Simon, C. Hauser and K. J. Wilkinson, Bioaccumulation and effects of CdTe/CdS quantum dots on *Chlamydomonas reinhardtii*-nanoparticles or the free ions?, *Environmental science & technology*, 2011, **45**, 7664-7669.
88. S. Gonzalo, I. Rodea-Palomares, F. Leganes, E. Garcia-Calvo, R. Rosal and F. Fernandez-Pinas, First evidences of PAMAM dendrimer internalization in microorganisms of environmental relevance: A linkage with toxicity and oxidative stress, *Nanotoxicology*, 2014, DOI: 10.3109/17435390.2014.969345, 1-13.
89. P. S. Low and S. Chandra, Endocytosis in plants, *Annual review of plant biology*, 1994, **45**, 609-631.
90. N. G. Irani and E. Russinova, Receptor endocytosis and signaling in plants, *Current opinion in plant biology*, 2009, **12**, 653-659.
91. Y. Wang, A.-J. Miao, J. Luo, Z.-B. Wei, J.-J. Zhu and L.-Y. Yang, Bioaccumulation of CdTe quantum dots in a freshwater alga *Ochromonas danica*: a kinetics study, *Environmental science & technology*, 2013, **47**, 10601-10610.
92. Y. Yue, X. Li, L. Sigg, M. J. Suter, S. Pillai, R. Behra and K. Schirmer, Interaction of silver nanoparticles with algae and fish cells: a side by side comparison, *Journal of nanobiotechnology*, 2017, **15**, 16.
93. S. Ma and D. Lin, The biophysicochemical interactions at the interfaces between nanoparticles and aquatic organisms: adsorption and internalization, *Environmental Science: Processes & Impacts*, 2013, **15**, 145-160.
94. M. C. Hoepflinger, M. Hoefflberger, A. Sommer, C. Hametner and I. Foissner, Clathrin in *Chara australis*: Molecular Analysis and Involvement in Charasome Degradation and Constitutive Endocytosis, *Frontiers in plant science*, 2017, **8**.
95. http://www.genome.jp/kegg-bin/show_pathway?cre04144, Endocytosis - *Chlamydomonas reinhardtii*, http://www.genome.jp/kegg-bin/show_pathway?cre04144.
96. E. Navarro, A. Baun, R. Behra, N. B. Hartmann, J. Filser, A.-J. Miao, A. Quigg, P. H. Santschi and L. Sigg, Environmental behavior and ecotoxicity of engineered nanoparticles to algae, plants, and fungi, *Ecotoxicology*, 2008, **17**, 372-386.
97. M. Ovečka, I. Lang, F. Baluška, A. Ismail, P. Illeš and I. Lichtscheidl, Endocytosis and vesicle trafficking during tip growth of root hairs, *Protoplasma*, 2005, **226**, 39-54.
98. C. Xie, J. Zhang, Y. Ma, Y. Ding, P. Zhang, L. Zheng, Z. Chai, Y. Zhao, Z. Zhang and X. He, *Bacillus subtilis* causes dissolution of ceria nanoparticles at the nano-bio interface, *Environmental Science: Nano*, 2019, **6**, 216-223.
99. Y. Ma, P. Zhang, Z. Zhang, X. He, J. Zhang, Y. Ding, J. Zhang, L. Zheng, Z. Guo and L. Zhang, Where does the transformation of precipitated ceria nanoparticles in hydroponic plants take place?, *Environmental science & technology*, 2015, **49**, 10667-10674.
100. C. Bertin, X. Yang and L. A. Weston, The role of root exudates and allelochemicals in the rhizosphere, *Plant and soil*, 2003, **256**, 67-83.
101. P. McManus, J. Hortin, A. J. Anderson, A. R. Jacobson, D. W. Britt, J. Stewart and J. E. McLean, Rhizosphere interactions between copper oxide nanoparticles and wheat root exudates in a sand matrix: Influences on copper bioavailability and uptake, *Environmental toxicology and chemistry*, 2018, **37**, 2619-2632.
102. Y. Huang, L. Zhao and A. A. Keller, Interactions, transformations, and bioavailability of nano-copper exposed to root exudates, *Environmental science & technology*, 2017, **51**, 9774-9783.
103. C. O. Dimkpa, J. E. McLean, N. Martineau, D. W. Britt, R. Haverkamp and A. J. Anderson, Silver nanoparticles disrupt wheat (*Triticum aestivum* L.) growth in a sand matrix, *Environmental science & technology*, 2013, **47**, 1082-1090.
104. L. Weston, in *Root ecology*, Springer, 2003, pp. 235-255.

105. A. Kawasaki, S. Donn, P. R. Ryan, U. Mathesius, R. Devilla, A. Jones and M. Watt, Microbiome and exudates of the root and rhizosphere of *Brachypodium distachyon*, a model for wheat, *PLoS One*, 2016, **11**, e0164533.
106. Y. Li and W. Shen, Morphology-dependent nanocatalysts: rod-shaped oxides, *Chemical Society Reviews*, 2014, **43**, 1543-1574.
107. J. M. López, A. L. Gilbank, T. García, B. Solsona, S. Agouram and L. Torrente-Murciano, The prevalence of surface oxygen vacancies over the mobility of bulk oxygen in nanostructured ceria for the total toluene oxidation, *Applied Catalysis B: Environmental*, 2015, **174**, 403-412.
108. P. Dhonukshe, F. Aniento, I. Hwang, D. G. Robinson, J. Mravec, Y.-D. Stierhof and J. Friml, Clathrin-mediated constitutive endocytosis of PIN auxin efflux carriers in *Arabidopsis*, *Current Biology*, 2007, **17**, 520-527.
109. D. G. Robinson, L. Jiang and K. Schumacher, The endosomal system of plants: charting new and familiar territories, *Plant physiology*, 2008, **147**, 1482-1492.
110. E. R. Larson, E. Van Zelm, C. Roux, A. Marion-Poll and M. R. Blatt, Clathrin Heavy Chain subunits coordinate endo-and exocytic traffic and affect stomatal movement, *Plant physiology*, 2017, **175**, 708-720.
111. S. Kitakura, S. Vanneste, S. Robert, C. Löffke, T. Teichmann, H. Tanaka and J. Friml, Clathrin mediates endocytosis and polar distribution of PIN auxin transporters in *Arabidopsis*, *The Plant Cell*, 2011, **23**, 1920-1931.

SUPPLEMENTARY MATERIAL

Internalization and toxicological mechanisms of uncoated and PVP-coated cerium oxide nanoparticles in the freshwater alga *Chlamydomonas reinhardtii*

Gerardo Pulido-Reyes^{1,*}, Sophie Marie Briffa², Jara Hurtado-Gallego¹, Tetyana Yudina³, Francisco Leganés¹, Victor Puentes³, Eugenia Valsami-Jones^b, Roberto Rosal^d, Francisca Fernández-Piñas¹

1 Departamento de Biología, Facultad de Ciencias, Universidad Autónoma de Madrid, Spain

2 School of Geography, Earth and Environmental Sciences, University of Birmingham, Birmingham, UK

3 Department Ciències Fisiològiques I, University of Barcelona, Barcelona, Spain

4 Departamento de Ingeniería Química, Universidad de Alcalá, Alcalá de Henares, Spain

* Corresponding author: gerardo.pulido@uam.es

Contents:

Figure S1. TEM images and EDX spectra of *C. reinhardtii* cells before (left column) and after (right column) the application of EDTA washing steps.

Figure S2. Characterization of the non-coated and coated CeO₂NPs used in this work. TEM image of CeO₂NP (A – scale bar: 50 nm), CeO₂NP10 (B), CeO₂NP40 (C) and CeO₂NP360 (D). UV-vis absorbance spectrum of CeO₂NP, CeO₂NP10, CeO₂NP40 and CeO₂NP360 shown in E, F, G and H, respectively. XRD spectra of CeO₂NP showing the characteristic peaks of CeO₂ crystals is shown in I (there was no good XRD data for PVP-coated nanoparticles due to the external presence of PVP as capping agent). Section J shows the nominal size and percentage of surface Ce³⁺/Ce⁴⁺ of CeO₂NPs calculated by X-Ray photoelectron spectroscopy. TEM and UV-Vis spectra of PVP-coated CeO₂NPs are reproduced from Briffa et al (2017) with permission from the Royal Society of Chemistry. Additional characterization of these NPs can be also found in the cited reference.

Figure S3. Biological effect of 72 h exposure to the three PVP used to synthesize the different CeO₂NPs on the growth of *C. reinhardtii*. Data are expressed as percentages of the value of untreated cells (mean ± standard deviation).

Figure S4. Biological effect of 72 h exposure to TMAOH used to stabilize the uncoated CeO₂NPs on the growth of *C. reinhardtii*. Data are expressed as percentages of the value of untreated cells (mean ± standard deviation).

Figure S5. Biological effect of 0.1 mg/L of CeO₂NP, CeO₂NP10, CeO₂NP40 and CeO₂NP360 on cell membrane integrity (A), cytoplasmic membrane potential (B) and metabolic activity (C) of *C. reinhardtii*.

Figure S6. Effect of 0.1 mg/L of CeO₂NPs on intracellular superoxide anion and hydrogen peroxide levels of *C. reinhardtii* by FCM using the fluorochrome HE (A) and DHR123 (B), respectively. Alterations derived of oxidative stress in mitochondria and intracellular lipid peroxidation are also shown in (C) and (D), respectively.

Figure S7. Effect of TMAOH (compound used to stabilize uncoated CeO₂NPs) at 0.1 mM (B), 1 mM (C) and 2.5 mM (D) on the cell membrane integrity of *C. reinhardtii*. A: control cells without TMAOH.

Figure S8. The effect of the different endocytic inhibitors towards chlorophyll a fluorescence of *C. reinhardtii*. CT: control. MDC: monodansylcadaverine. EIPA: 5-(Nethyl-N-isopropyl)-amiloride. NaN₃: Sodium azide.

Figure S9. Level of reduction of intracellular CeO₂NPs after the treatment with the MDC inhibitor. Data are expressed as percentage of reduction in comparison with CNPs samples without inhibitor (mean ± standard deviation).

Figure S10. Effect of CeO₂NPs on expression of CHC1 gene after 4 h of exposure. Data are represented as relative expression of the genes with respect to the unexposed control. Control values were set to 1 for easy comparison.

Table S1. Fluorochromes used in this work.

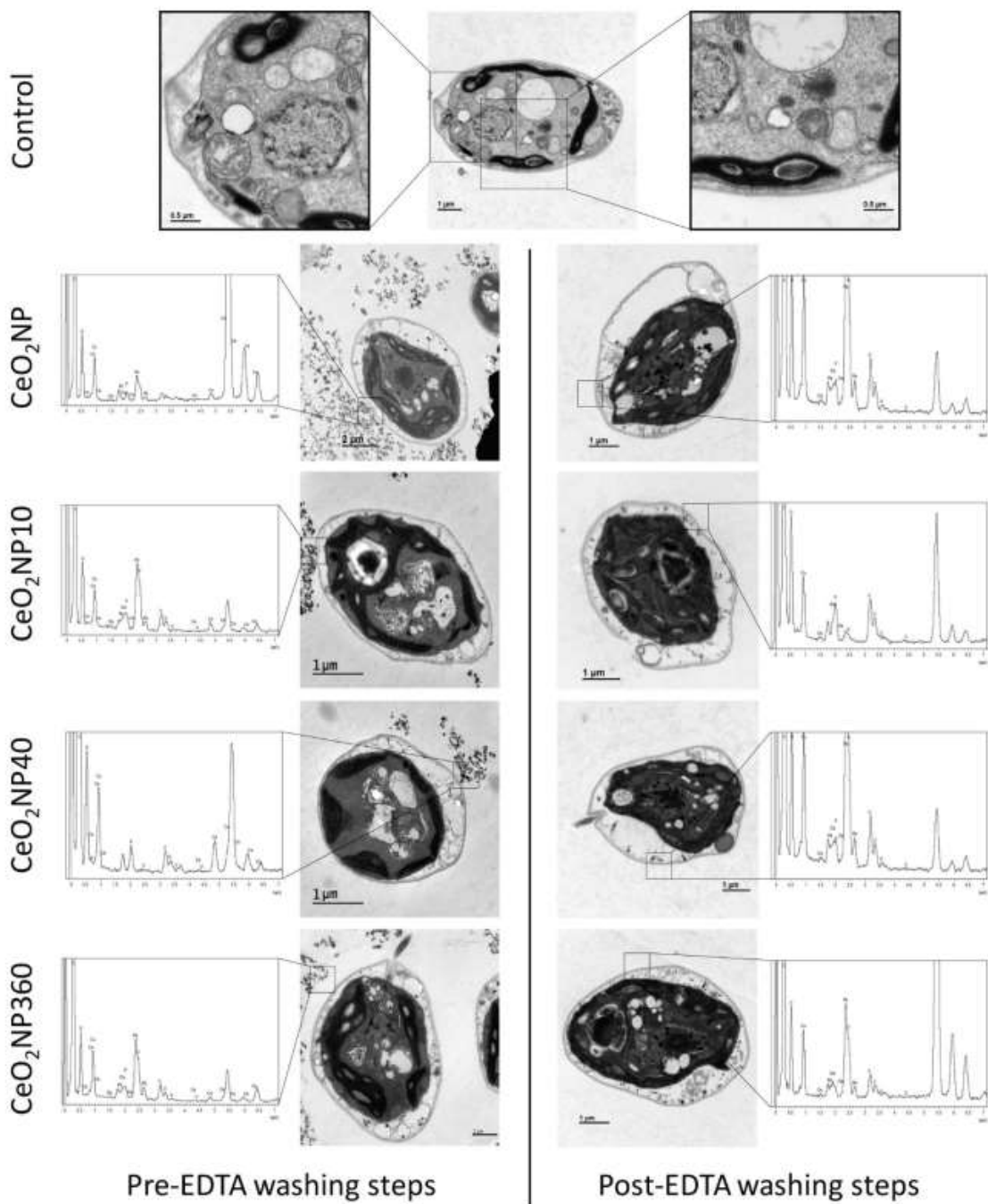


Figure S1. TEM images and EDX spectra of *C. reinhardtii* cells before (left column) and after (right column) the application of EDTA washing steps.

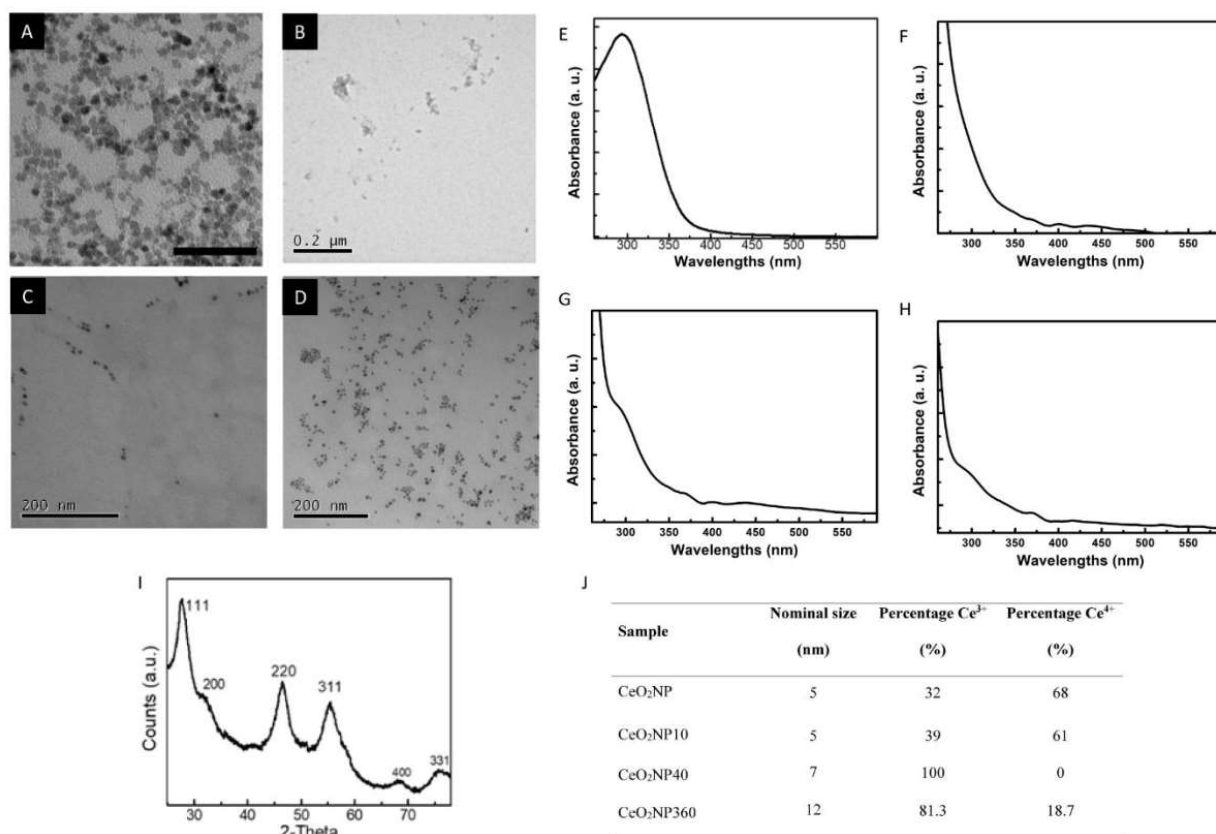


Figure S2. Characterization of the non-coated and coated CeO₂NPs used in this work. TEM image of CeO₂NP (A – scale bar: 50 nm), CeO₂NP10 (B), CeO₂NP40 (C) and CeO₂NP360 (D). UV-vis absorbance spectrum of CeO₂NP, CeO₂NP10, CeO₂NP40 and CeO₂NP360 shown in E, F, G and H, respectively. XRD spectra of CeO₂NP showing the characteristics peaks of CeO₂ crystals is shown in I (there was no good XRD data for PVP-coated nanoparticles due to the external presence of PVP as capping agent). Section J shows the nominal size and percentage of surface Ce³⁺/Ce⁴⁺ of CeO₂NPs calculated by X-Ray photoelectron spectroscopy. TEM and UV-Vis spectra of PVP-coated CeO₂NPs are reproduced from Briffa et al (2017) with permission from the Royal Society of Chemistry. Additional characterization of these NPs can be also found in the cited reference.

Reference: Briffa, S. M., Lynch, I., Trouillet, V., Bruns, M., Hapiuk, D., Liu, J., ... & Valsami-Jones, E. (2017). Development of scalable and versatile nanomaterial libraries for nanosafety studies: polyvinylpyrrolidone (PVP) capped metal oxide nanoparticles. *RSC Advances*, 7(7), 3894-3906.

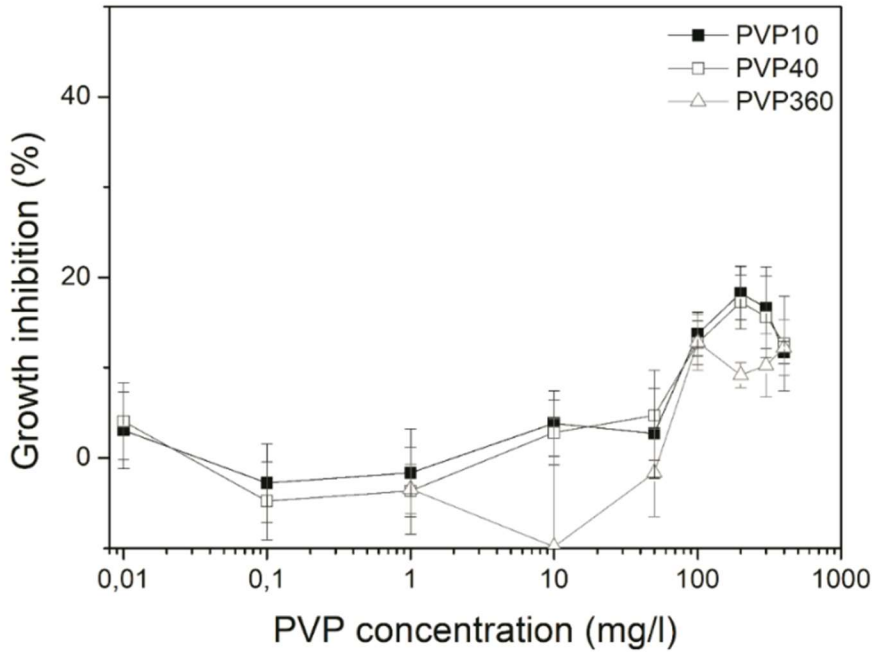


Figure S3. Biological effect of 72 h exposure to the three PVP used to synthesize the different CeO₂NPs on the growth of *C. reinhardtii*. Data are expressed as percentages of the value of untreated cells (mean ± standard deviation).

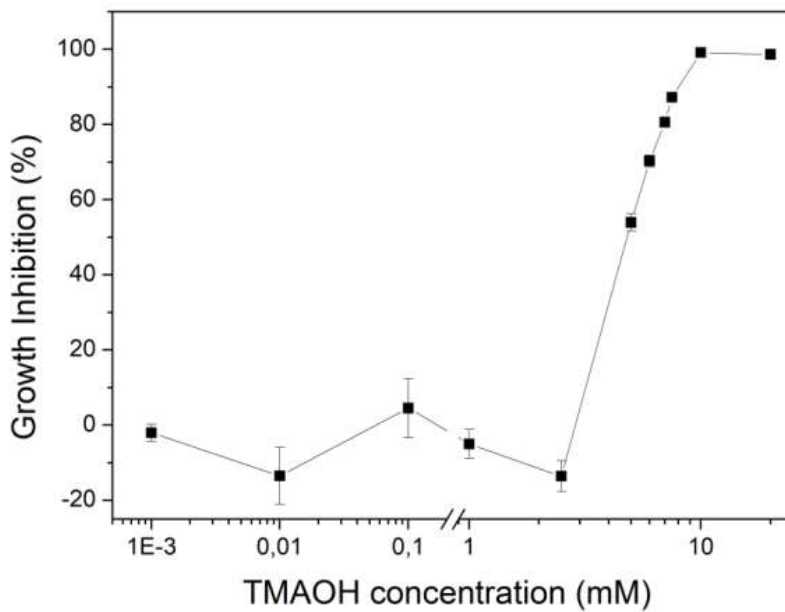


Figure S4. Biological effect of 72 h exposure to TMAOH used to stabilize the uncoated CeO₂NPs on the growth of *C. reinhardtii*. Data are expressed as percentages of the value of untreated cells (mean ± standard deviation).

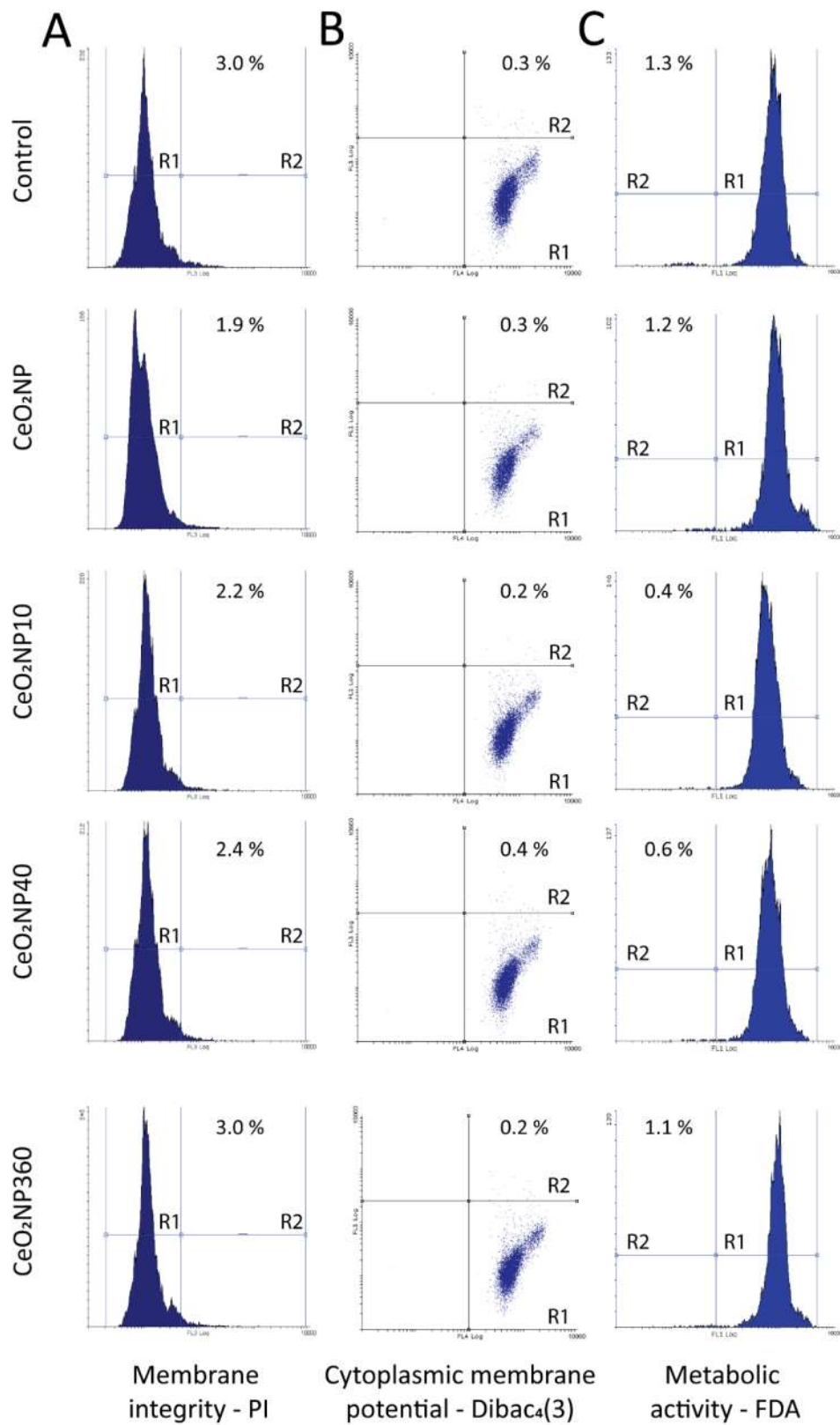


Figure S5. Biological effect of 0.1 mg/L of CeO₂NP, CeO₂NP10, CeO₂NP40 and CeO₂NP360 on cell membrane integrity (A), cytoplasmic membrane potential (B) and metabolic activity (C) of *C. reinhardtii*.

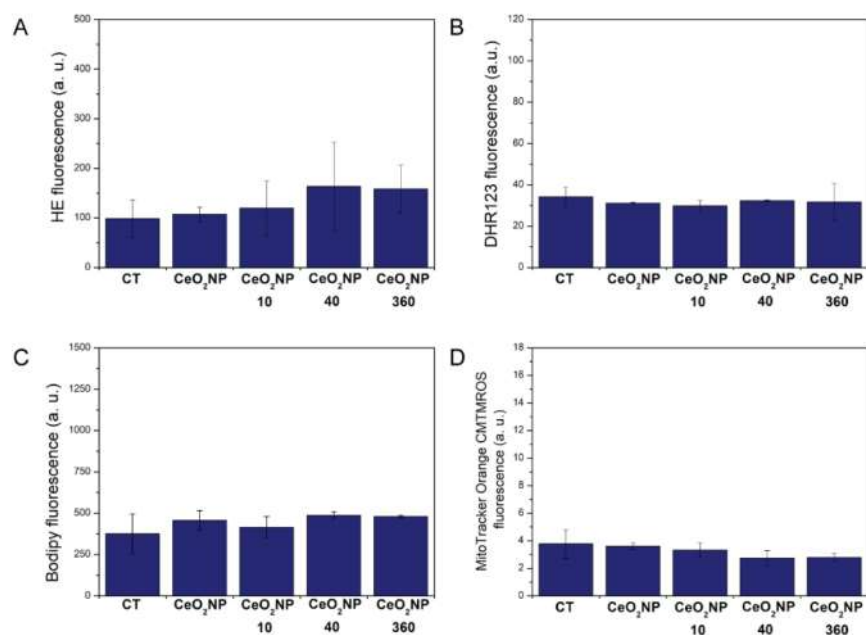


Figure S6. Effect of 0.1 mg/L of CeO₂NPs on intracellular superoxide anion and hydrogen peroxide levels of *C. reinhardtii* by FCM using the fluorochrome HE (A) and DHR123 (B), respectively. Alterations derived of oxidative stress in mitochondria and intracellular lipid peroxidation are also shown in (C) and (D), respectively.

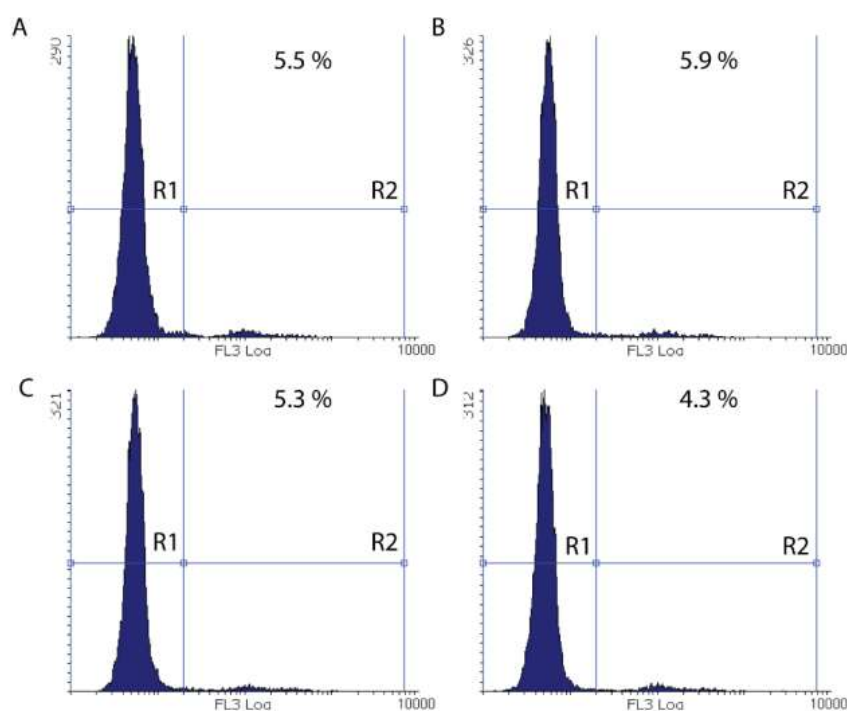


Figure S7. Effect of TMAOH (compound used to stabilize uncoated CeO₂NPs) at 0.1 mM (B), 1 mM (C) and 2.5 mM (D) on the cell membrane integrity of *C. reinhardtii*. A: control cells without TMAOH.

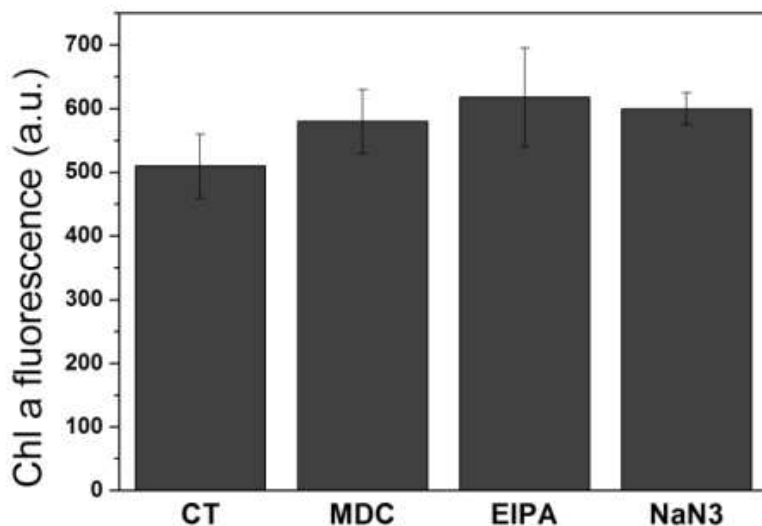


Figure S8. The effect of the different endocytic inhibitors towards chlorophyll a fluorescence of *C. reinhardtii*. CT: control. MDC: monodansylcadaverine. EIPA: 5-(Nethyl-N-isopropyl)-amiloride. NaN3: Sodium azide.

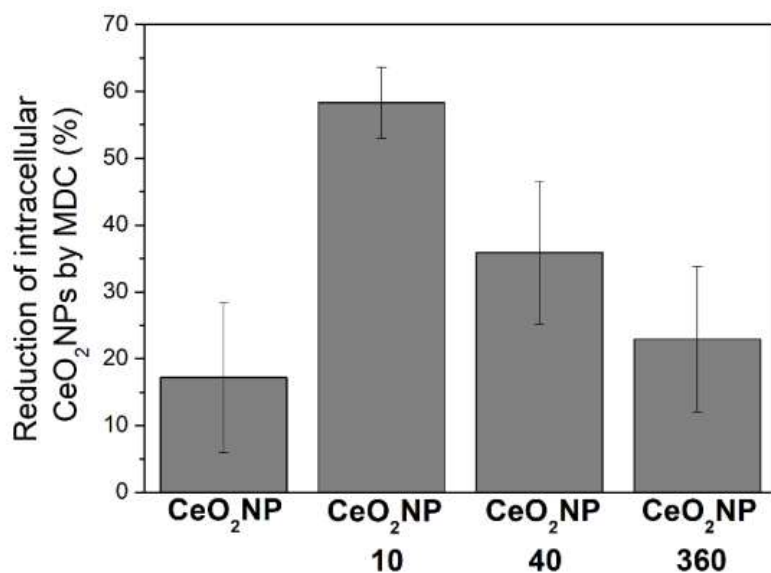


Figure S9. Level of reduction of intracellular CeO₂NPs after the treatment with the MDC inhibitor. Data are expressed as percentage of reduction in comparison with CNPs samples without inhibitor (mean ± standard deviation).

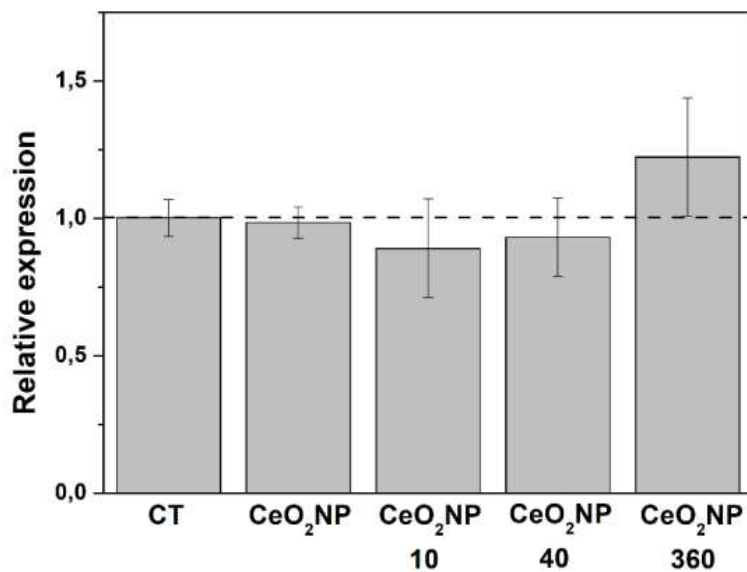


Figure S10. Effect of CeO₂NPs on expression of CHC1 gene after 4 h of exposure. Data are represented as relative expression of the genes with respect to the unexposed control. Control values were set to 1 for easy comparison.

Table S1. Fluorochromes used in this work.

Fluorochrome	Acronym	Applications	Stock concentration (mg mL ⁻¹)	Final concentration (µg mL ⁻¹)	Incubation time (min)
Dihydrorhodamine 123	DHR 123	Intracellular levels of hydrogen peroxide	2	10	40
Hydroethidine	HE	Intracellular levels of superoxide anion	3.154	5	30
Propidium iodide	IP	Membrane integrity	1	5	10
Fluorescein Diacetate	FDA	Unspecific esterase activity	5	2.5	15
bis-(1,3-dibutylbarbituric acid) trimethine oxonol	DiBAC₄(3)	Cytoplasmic membrane potential	0.5	2.5	10
5-Butyl-4,4-Difluoro-4-Bora-3a,4a-Diaza-s-Indacene-3-Nonanoic Acid	BODIPY- C4-C9	Lipid peroxidation	101.08	0.01	10
MitoTracker® Orange CM-H2TMRos	Mitotracker	Mitochondrial ROS homeostasis	0.05	2.5	60